NASA TECHNICAL NOTE

(NASA TN D-1993)

46p.

N63 22601

CODE-1

NASA TN D-1993

MAGNETIC FIELD OF A FINITE HELICAL SOLENOID

by A. R. Sass and James C. Stoll

Lewis Research Center

Cleveland, Ohio

NATIONAL AERONAUTICS AND SPACE ADMINISTRATION • WASHINGTON, D.C. • OCTOBER 1963

TECHNICAL NOTE D-1993

MAGNETIC FIELD OF A FINITE HELICAL SOLENOID

By A. R. Sass and James C. Stoll

Lewis Research Center
Cleveland, Ohio

NATIONAL AERONAUTICS AND SPACE ADMINISTRATION

MAGNETIC FIELD OF A FINITE HELICAL SOLENOID

By A. R. Sass and James C. Stoll

SUMMARY

22601

A superposition principle was utilized to calculate the magnetic field distribution of a solenoid of finite length with infinitely thin walls wound with a finite helical angle. This field distribution is the vector sum of the distributions due to the azimuthal and axial components of the current density. The magnetic fields are expressed in terms of tabulated solutions of complete elliptic integrals, and they are presented in graphical form for values of helical angles from 5° to 45° and values of the ratio of solenoid length to radius from 1 to 20.

AUTHOR

INTRODUCTION

A form of the Stellarator, as defined in reference 1, is one example of magnetic field source geometries in which current flows in a helical path. The magnetic field distribution of this Stellarator has been calculated only approximately because of the difficulty in evaluating the Biot-Savart integral expressions associated with its solution (ref. 1). Even the approximations that have been made are based on the assumption of infinite length, and therefore the desired field distribution can at best be obtained by "cut and try" experimental techniques. The magnetic field distribution of the N-wire Stellarator discussed in reference 1 is given in a series expression for which a closed-form solution has not yet been found. Another geometry that will produce a field similar to the N-wire Stellarator, however, is a helical solenoid of finite length. An added advantage of this geometry is that it may be analyzed mathematically if the idealized assumptions that are stated in the section STATEMENT OF PROBLEM are used. Another feature of such a geometry is that it is the basic building block of a relatively force-free solenoid (ref. 2).

An analysis of the field distribution of this solenoid is presented and a general technique by which the Lorentz force on the solenoid walls can be evaluated is described in this report.

SYMBOLS

The rationalized meter-kilogram-second system of units is used herein.

a solenoid radius

$\vec{b}$ unit vector in helical direction

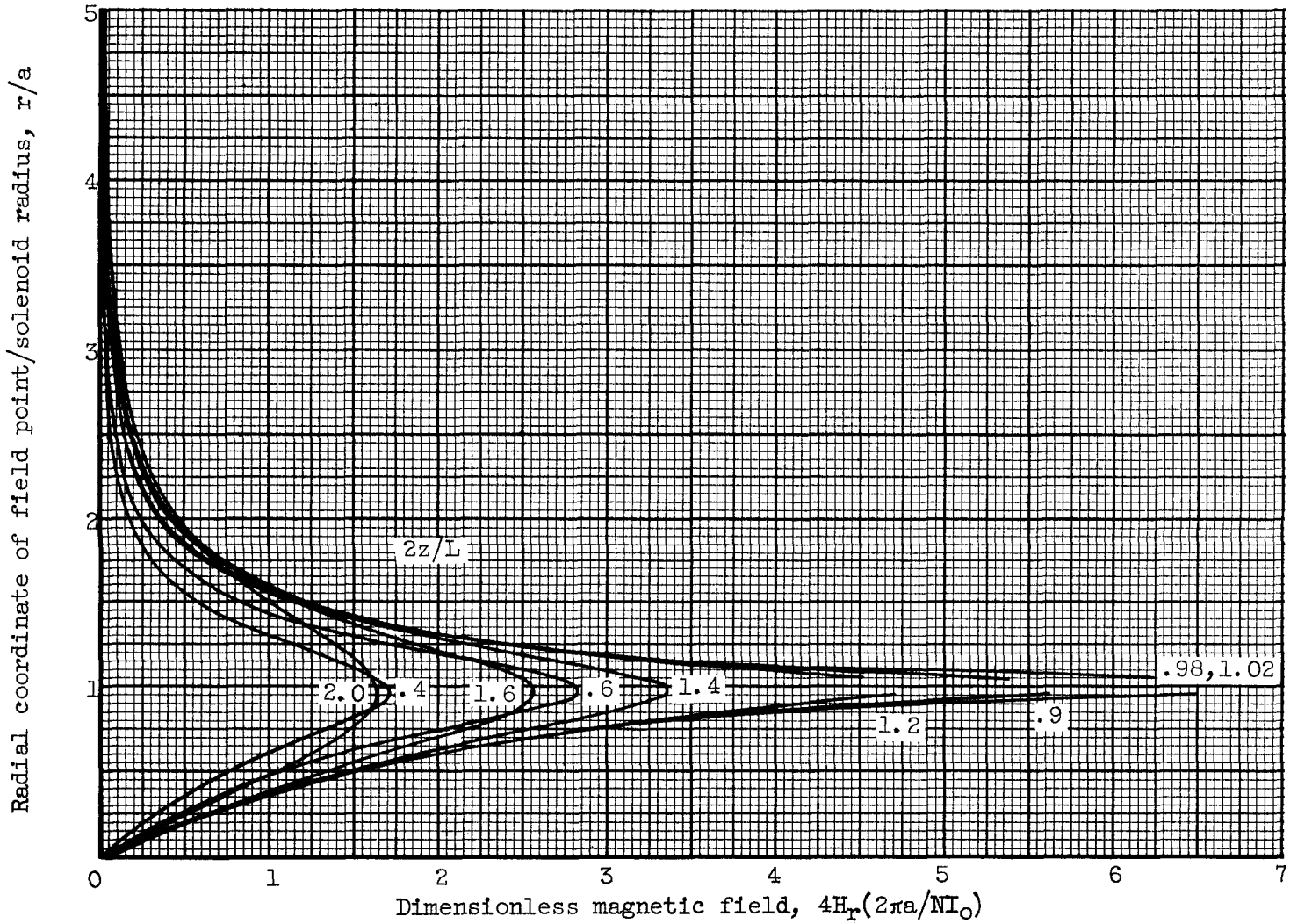

(e) Helical angle, 15.0°; length-radius ratio, 1.0.

Figure 2. - Continued. Dimensionless radial field of helical solenoid.

$\vec{ds}$	differential element of solenoid circumference
$E(k)$	elliptic integral of second kind
H_r	radial magnetic field intensity
H_z	axial magnetic field intensity
H_θ	azimuthal magnetic field intensity
I_o	current per wire
J	current per unit width in helical direction
J_z	current per unit width in axial direction
J_θ	current per unit width in azimuthal direction
j	current density in helical direction
$K(k)$	elliptic integral of the first kind
k^2	$4ar/\left[\xi^2 + (a + r)^2\right]$
L	solenoid length
N	number of solenoid wires
p	Lorentz pressure
r	radial coordinate of field point
Sn u	Jacobian elliptic function
S_1	cross-sectional area of solenoid
z	axial coordinate of field point
z_o	axial coordinate of source point
α	helical angle
θ	angular coordinate of source point
$\lambda_o(\varphi,k)$	Heuman lambda function
μ_o	magnetic permeability of free space
ξ	dummy variable of integration
$\xi_\pm$	$z \pm L/2$

$\varphi \quad \tan^{-1} \mid \xi/(a - r) \mid$

Superscript:

$\rightarrow$ denotes vector

STATEMENT OF PROBLEM

Sketch (a) illustrates a typical helical solenoid of length L, radius a, helical angle α, and N wires. Two high-conductivity metal collars are provided

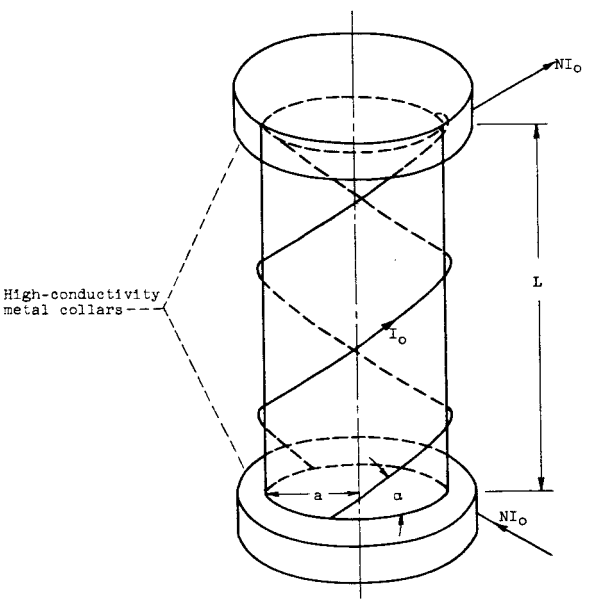

(a) N-Wire finite helical solenoid.

to introduce the current uniformly into the N wires. If the wires are superconductors (zero electrical resistance), the current will not necessarily be introduced into the N wires uniformly, since the current distribution is influenced by the inductance of each current path. If the lead-in wires are connected to the geometrical centers of the collars (which may also be superconductors if desired), the inductance of the current paths are all identical and the current is uniformly introduced into the N wires.

For the sake of simplicity, it will be assumed that a large number N of extremely thin wires are evenly distributed over and completely cover the cylinder surface. The solenoid can then be approximated by a current sheet (sketch (b)). The contribution to the field distribution of the current in the

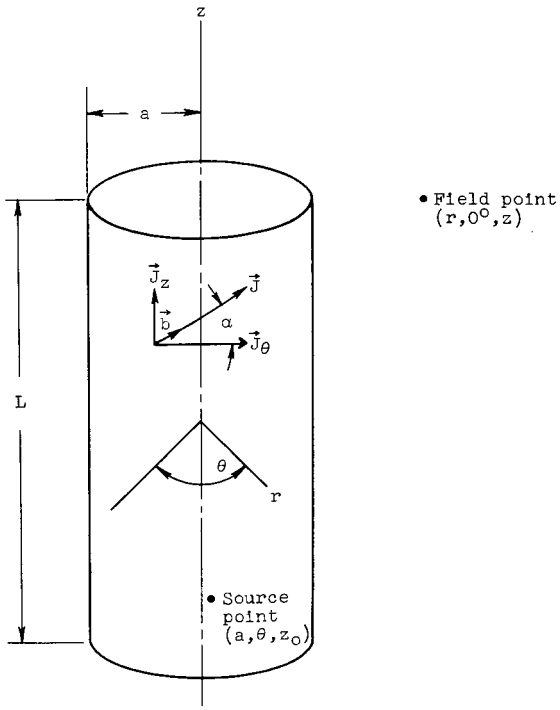

(b) Mathematical idealization of N-wire helical solenoid.

metal collars and the lead-in wires will be neglected in the following analysis. The error incurred by such an approximation is examined in the DISCUSSION.

At this point, it is convenient to define a current per unit width $\vec{J}$ in the helical direction that is defined by the unit vector $\vec{b}$.

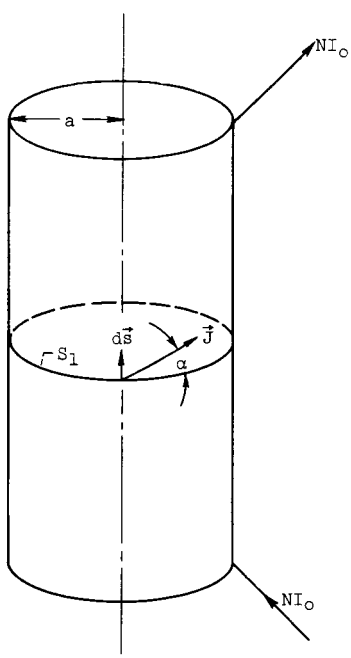

(c) Model used to define $\vec{J}$.

For a steady-state condition (sketch (c)),

$$\int_{S_1} \vec{j} \cdot \vec{ds} = \int_0^{2\pi} J \sin \alpha \, a d\theta = NI_o \tag{1a}$$

Since j and α are independent of θ,

$$J = \frac{NI_o}{2\pi a \sin \alpha} \tag{1b}$$

Although $\vec{J}$ is singular for $\alpha = 0$, this case is not physically realizable for the N-wire solenoid.

The magnetic field distribution can be obtained either by using the Biot-Savart law or by defining the vector potential and performing the necessary curl operation. The Biot-Savart law is used throughout this report.

The Biot-Savart law is a linear vector equation that yields an analytic expression for the magnetic field at all points except the source point. The magnetic field distribution is thus equal to the vector sum of the fields due to a sheet of azimuthal current flow and a sheet of axial current flow. The current per unit width $\vec{J}$ can be resolved into an azimuthal compount J_θ and an axial component J_z, such that

$$J_\theta = J \cos \alpha \tag{2a}$$

$$J_z = J \sin \alpha \tag{2b}$$

Reference to equation (1) shows that J_z is independent of α. This is physically reasonable since the net axial current flow must be equal to NI_o.

FIELD DISTRIBUTION FOR AZIMUTHAL CURRENT

From an investigation of the field distribution of the azimuthal current flow (ref. 3) the radial field H_r and the axial field H_z are

$$H_r(r,z) = \frac{J_\theta}{\pi}\left(\frac{a}{r}\right)^{1/2}\left[\frac{2 - k^2}{2k} K(k) - \frac{E(k)}{k}\right]_{\xi_-}^{\xi_+} \tag{3a}$$

and

$$H_z(r,z) = \frac{J_\theta}{4}\left[\frac{\xi k}{\pi(ar)^{1/2}} K(k) + \frac{(a - r)\xi}{|(a - r)\xi|} \lambda_o(\varphi,k)\right]_{\xi_-}^{\xi_+} \tag{3b}$$

where $K(k)$ and $E(k)$ are the complete elliptic integrals of the first and second kind, respectively. From reference 4, $k^2 = \frac{4ar}{\xi^2 + (a + r)^2}$,

$\varphi = \tan^{-1}\left|\frac{\xi}{a - r}\right|$, $\xi_\pm = z \pm \frac{L}{2}$, and $\lambda_o(\varphi,k)$ is the Heuman lambda function.

As $r \to 0$, these expressions reduce to the standard result for the field along the axis:

$$H_r = \frac{J_\theta}{4}\left[\frac{a^2 r}{(\xi^2 + a^2)^{3/2}}\right]_{\xi_-}^{\xi_+} \tag{3c}$$

and

$$H_z = \frac{J_\theta}{2}\left[\frac{\xi}{(\xi^2 + a^2)^{1/2}}\right]_{\xi_-}^{\xi_+} \tag{3d}$$

FIELD DISTRIBUTION FOR AXIAL CURRENT

The azimuthal magnetic field for the axial current is given by the Biot-Savart law:

$$H_\theta(r,z) = \frac{J_z a}{2\pi}\int_0^\pi \int_{-L/2}^{L/2} \frac{(r - a\cos\theta)dz_o\, d\theta}{\left[(z - z_o)^2 + r^2 + a^2 - 2ar\cos\theta\right]^{3/2}} \tag{4}$$

where z_o is the axial coordinate of the source point (sketch (b)). Making a change of variables $\xi = z - z_o$ and integrating with respect to ξ yield

$$H_\theta(r,z) = \frac{J_z a}{2\pi} \int_0^\pi \left[\frac{\xi(r - a\cos\theta)d\theta}{(r^2 + a^2 - 2ar\cos\theta)(\xi^2 + r^2 + a^2 - 2ar\cos\theta)^{1/2}} \right]_{\xi_-}^{\xi_+} \tag{5}$$

Introducing a change of variables $t = \cos\theta$ and integrating with respect to t yield successively

$$H_\theta = \frac{J_z\left(\frac{r}{a}\right)^{1/2}}{4\pi(r + a)^{1/2}} \left[\xi k \int_0^{K(k)} \frac{1 - \frac{2a}{a + r} Sn^2 u}{1 - \frac{4ar}{(a + r)^2} Sn^2 u} du \right]_{\xi_-}^{\xi_+} \tag{6}$$

and

$$H_\theta = \frac{J_Z}{4} \left[\frac{\xi k}{\pi(ar)^{1/2}} K(k) + \frac{(r - a)\xi}{|(r - a)\xi|} \lambda_o(\varphi,k) \right]_{\xi_-}^{\xi_+} \tag{7}$$

(ref. 4, formulas 233.19 and 413.06), where Sn u is the Jacobian elliptic function. On the axis $r = 0$, equation (7) reduces to zero.

The total magnetic field distribution of the current sheet with finite helical angle α is given by equations (3) and (7), where J_θ and J_Z are given by equations (1) and (2).

DISCUSSION

The dimensionless magnetic field $4H_i(2\pi a/NI_o)$, where $i = r$, z, or θ depending on the field being discussed, is plotted as a function of the helical angle α and the dimensionless parameters $2z/L$ and r/a. (The azimuthal, radial, and axial fields are given in figures 1, 2, and 3, respectively.) The fields are given for (1) $\alpha = 5^\circ$, 15°, 30°, and 45°; (2) $L/a = 1$, 5, 10, and 20; and (3) $r/a \leq 5$.

The azimuthal field inside the solenoid $(r/a) < 1$ is small. It is the same order of magnitude as the field due to the current in the solenoid collars and the solenoid lead-in wires (the latter field was neglected in the analysis). In a physical situation, the fields due to the current in the collars and lead-in wires must be included.

The radial field is infinite at $r = a$ and $z = \pm L/2$ (edge of the cylinder) because of the thin current sheet idealization that results in a magnetic field with zero radius of curvature at the cylinder edge. For actual nonzero sheet thickness, this effect would not occur.

In addition to being used to provide an azimuthal field, the helically wound solenoid can be used to achieve a relatively force-free magnet. If ΔH_θ is the discontinuity of the azimuthal field at the current sheet surface (fig. 1) and ΔH_z is the discontinuity of the axial field (fig. 3), the net Lorentz pressure on the sheet surface is

$$p = \frac{\mu_o}{2} \left(J_\theta \, \Delta H_z - J_z \, \Delta H_\theta\right)$$

As is pointed out in reference 2, for $L = \infty$, the net pressure is zero for a helical angle of 45°. As reference 2 further indicates, however, this condition is not really force-free since in an actual coil the wires are subjected to equal but opposite Lorentz forces that may destroy the wires if large currents are used. This condition can be alleviated by building up layers of helical windings and letting α vary from approximately 0° to 90°. The analytic results presented herein can be used to calculate the forces on such a structure and the magnetic field distribution for the case of finite length if the solenoid wall thickness is much smaller than the solenoid radius.

Lewis Research Center
National Aeronautics and Space Administration
Cleveland, Ohio, July 11, 1963

REFERENCES

1. Aleksin, V. F.: On the Calculation of the Magnetic Field of the Stellarator. Soviet Phys.-Tech. Phys., vol. 6, no. 11, May 1962, pp. 934-936.

2. Furth, Harold P., Levine, Morton A., and Waniek, Ralph W.: Strong Magnetic Fields. Scientific Am., vol. 198, no. 2, Feb. 1958, pp. 28-33.

3. Callaghan, Edmund E., and Maslen, Stephen H.: The Magnetic Field of a Finite Solenoid. NASA TN D-465, 1960.

4. Byrd, Paul F., and Friedman, Morris D.: Handbook of Elliptic Integrals for Engineers and Physicists. Springer-Verlag (Berlin), 1954.

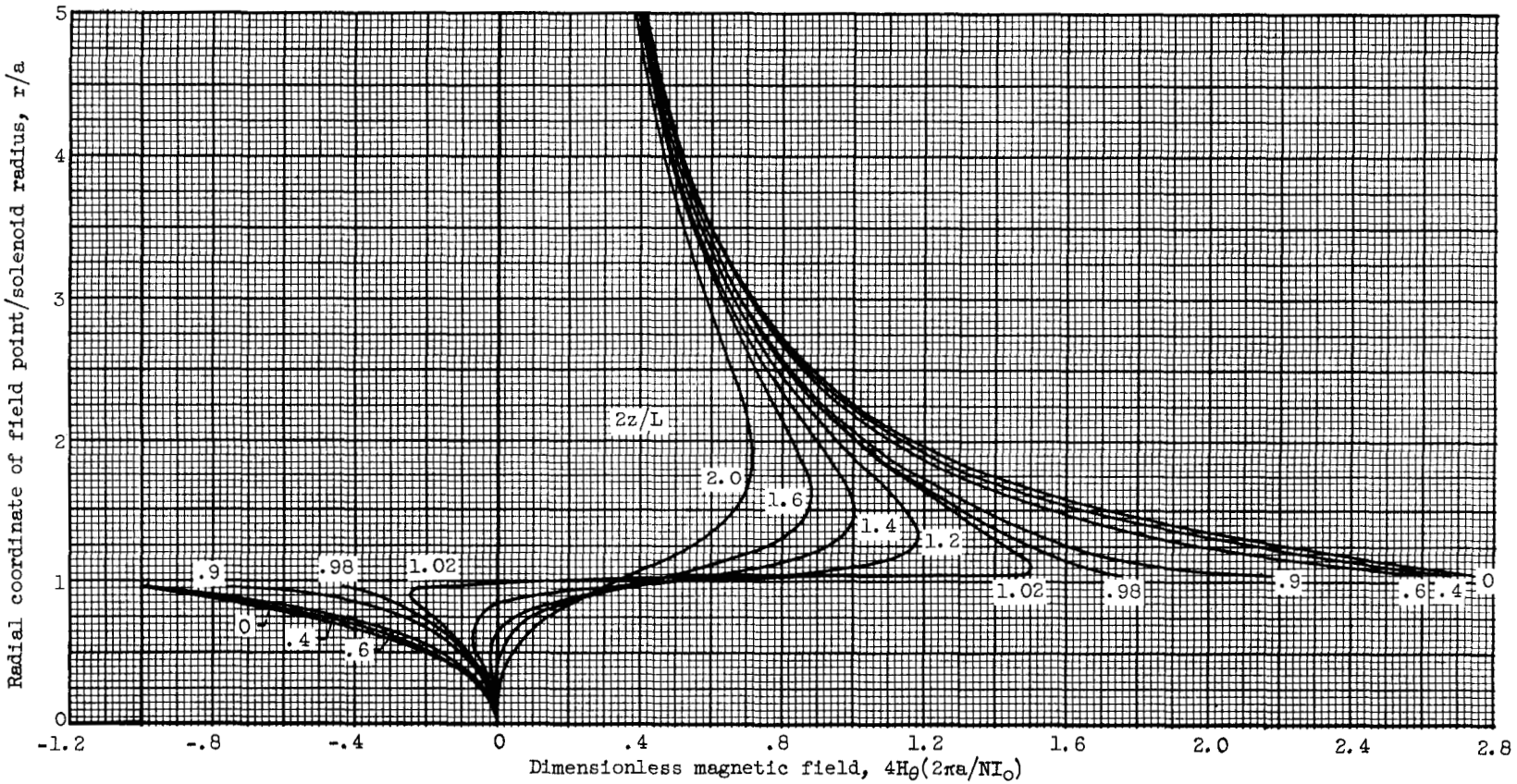

(a) Length-radius ratio, 1.0.

Figure 1. - Dimensionless azimuthal field of helical solenoid.

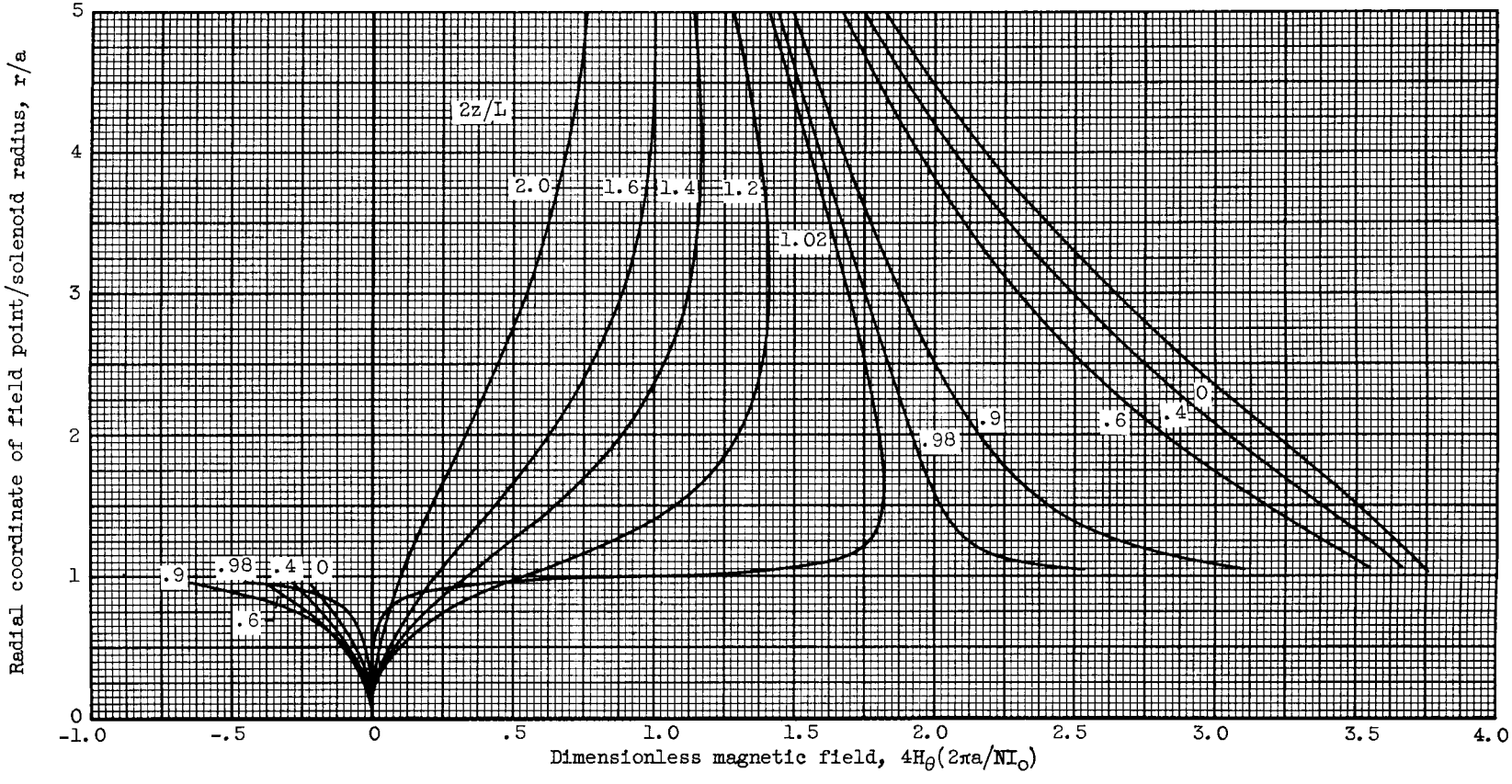

(b) Length-radius ratio, 5.0.

Figure 1. - Continued. Dimensionless azimuthal field of helical solenoid.

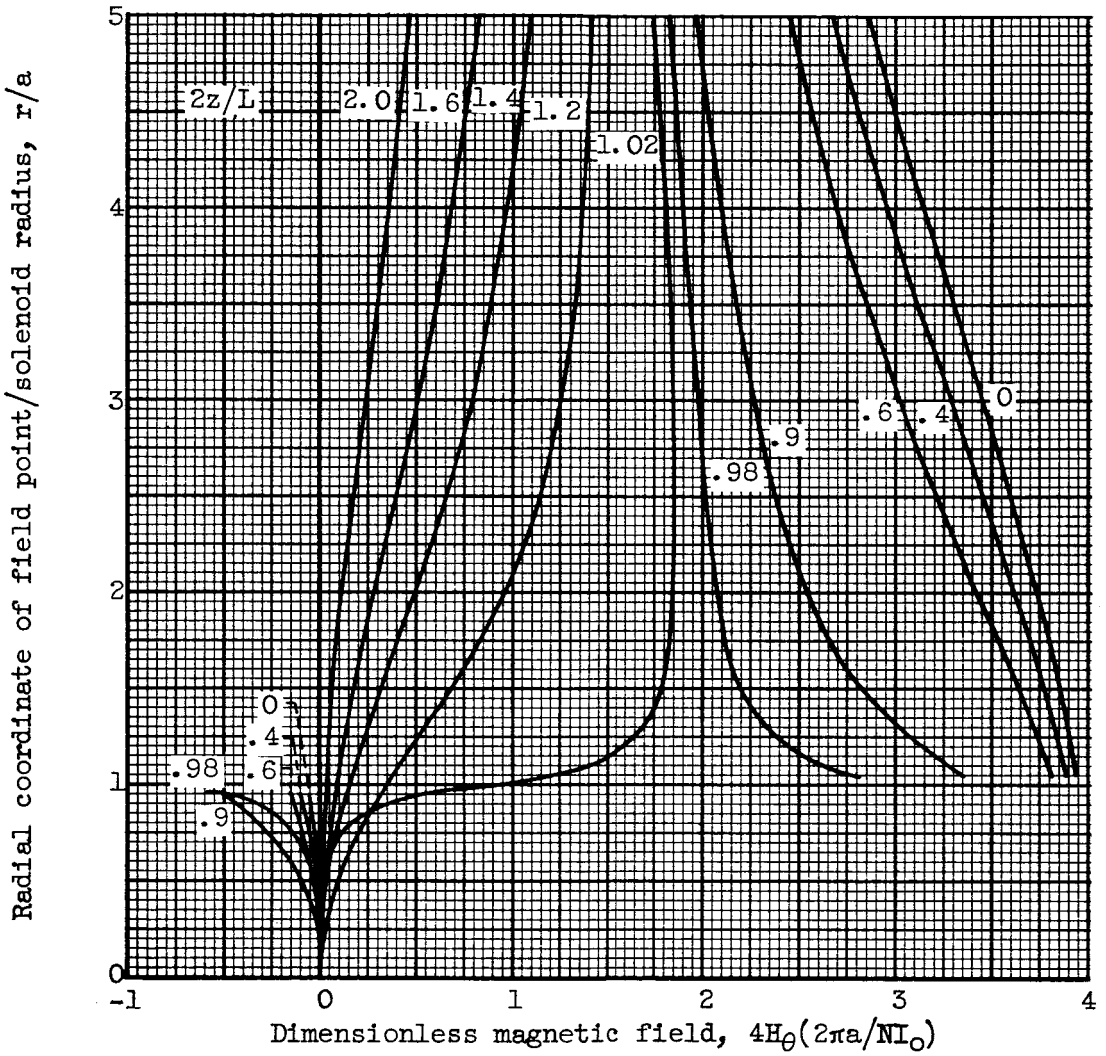

(c) Length-radius ratio, 10.0.

Figure 1. - Continued. Dimensionless azimuthal field of helical solenoid.

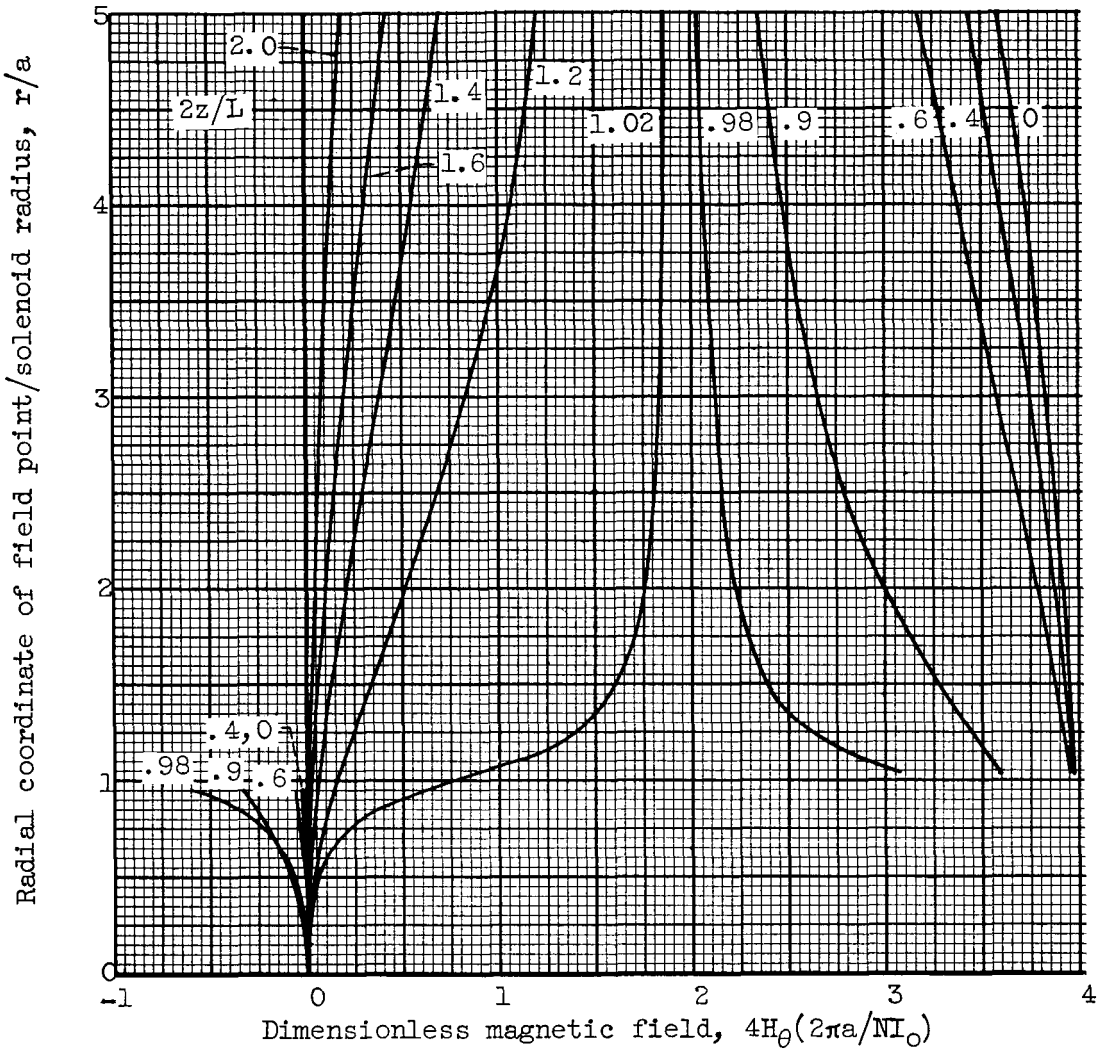

(d) Length-radius ratio, 20.0.

Figure 1. - Concluded. Dimensionless azimuthal field of helical solenoid.

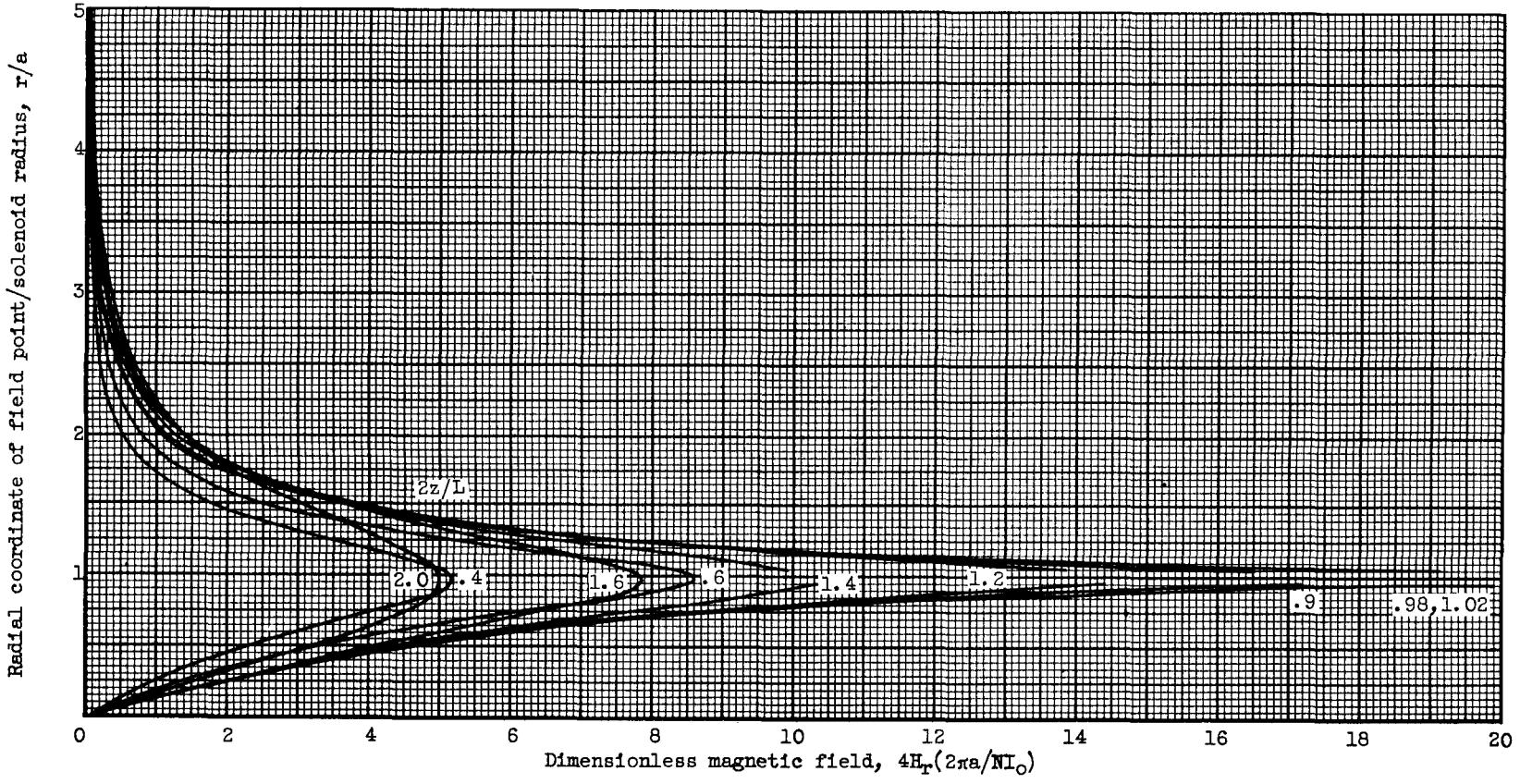

(a) Helical angle, 5.0°; length-radius ratio, 1.0.

Figure 2. - Dimensionless radial field of helical solenoid.

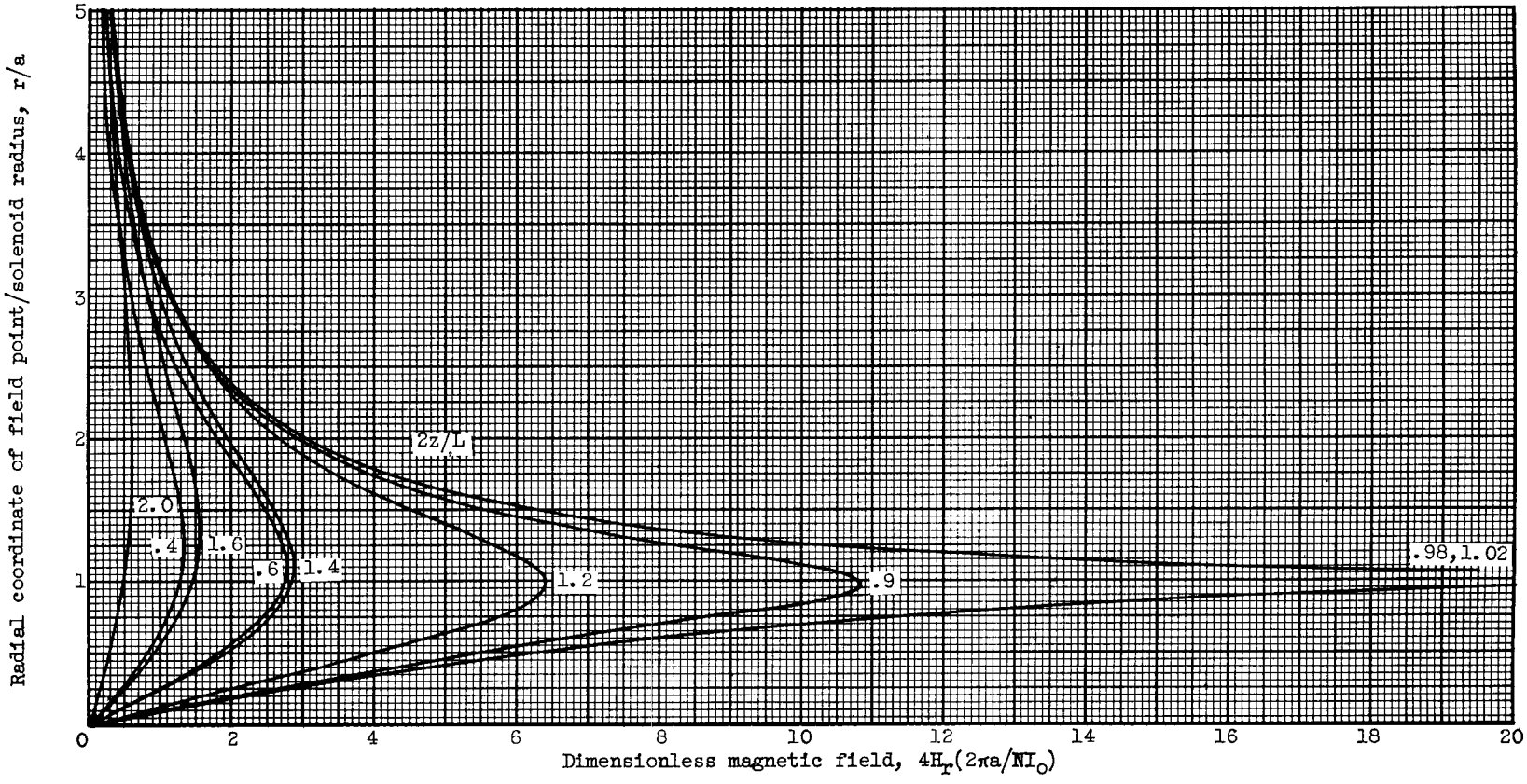

(b) Helical angle, 5.0°; length-radius ratio, 5.0.

Figure 2. - Continued. Dimensionless radial field of helical solenoid.

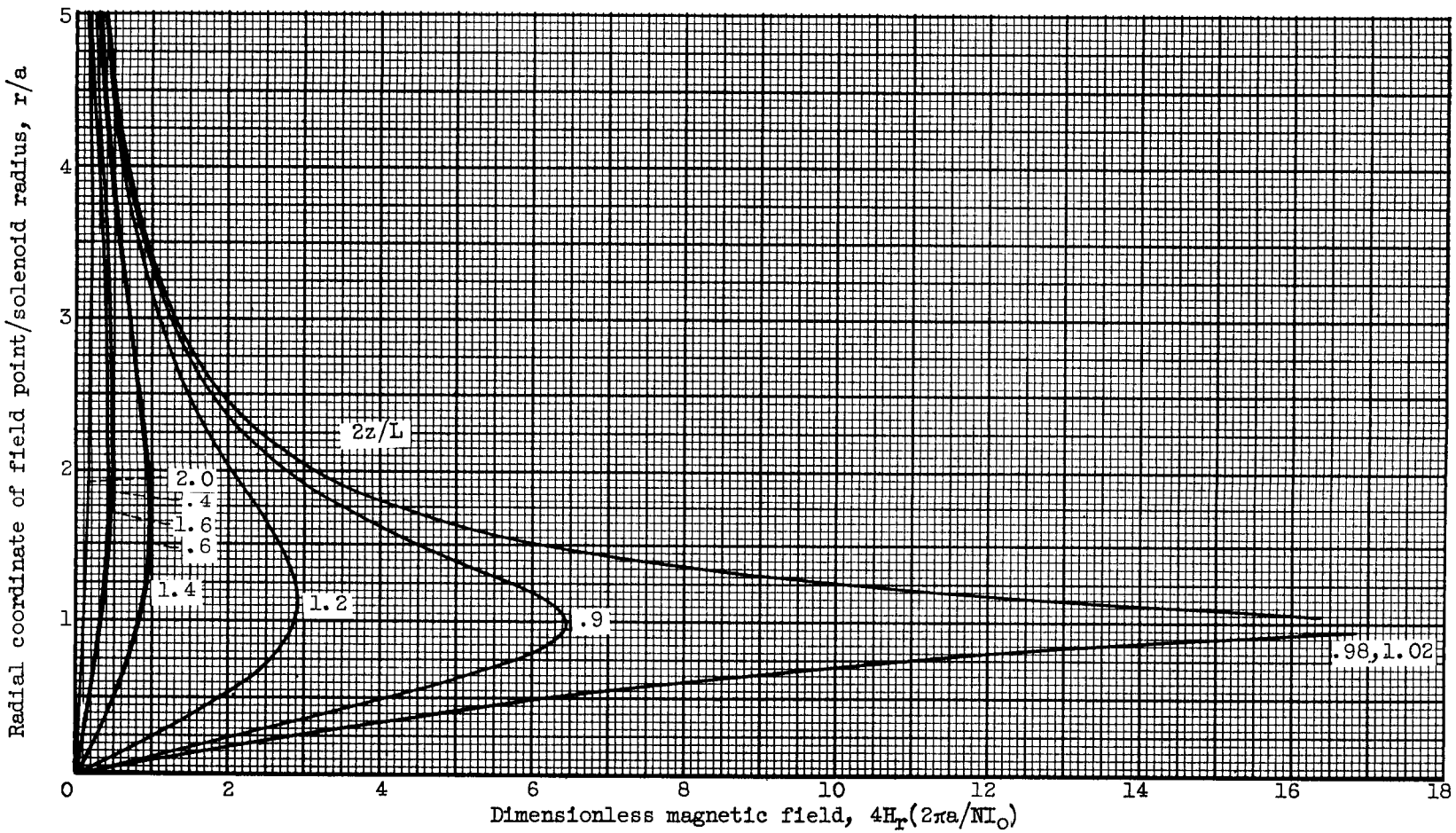

(c) Helical angle, 5.0°; length-radius ratio, 10.0.

Figure 2. - Continued. Dimensionless radial field of helical solenoid.

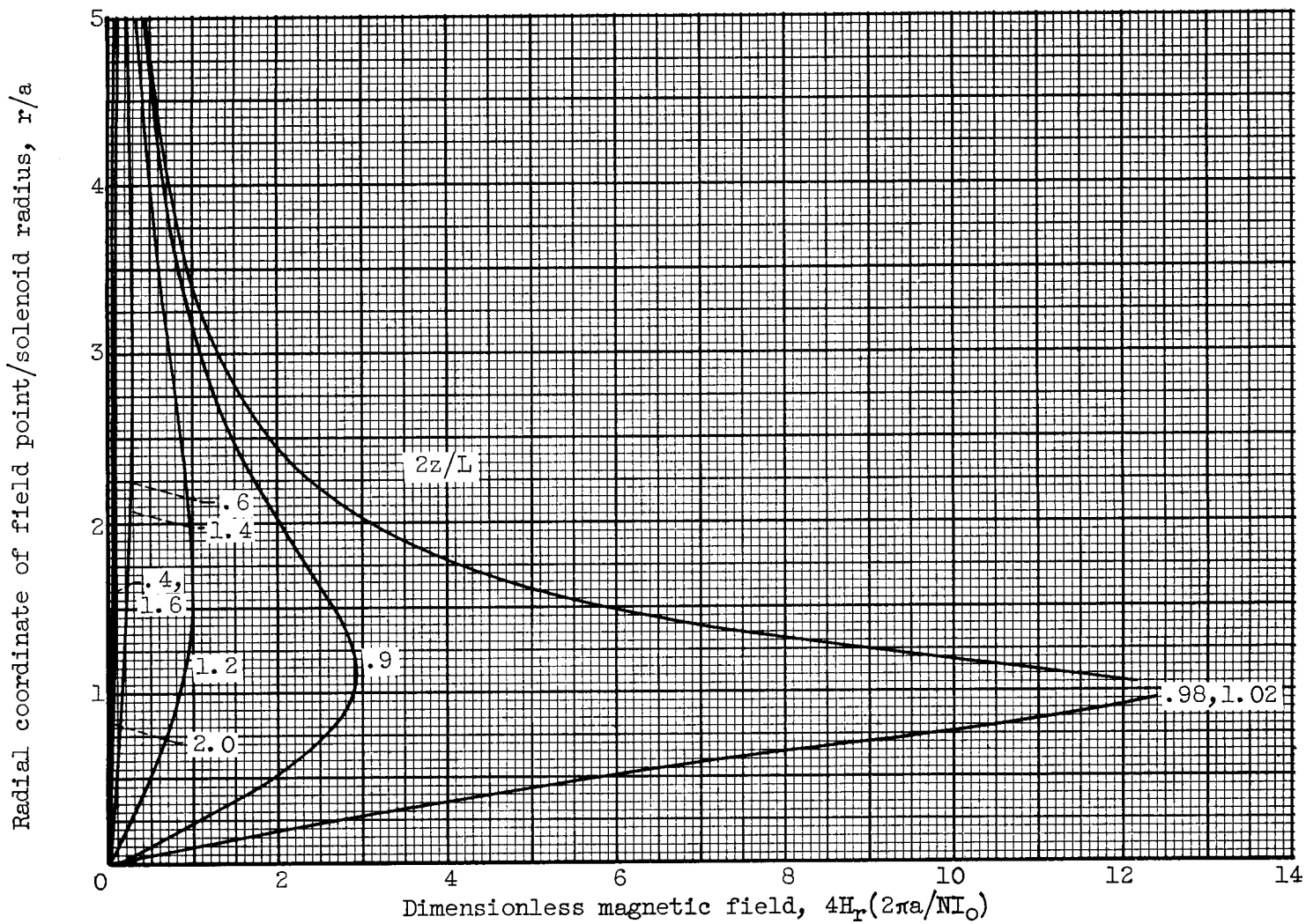

(d) Helical angle, 5.0°; length-radius ratio, 20.0.

Figure 2. - Continued. Dimensionless radial field of helical solenoid.

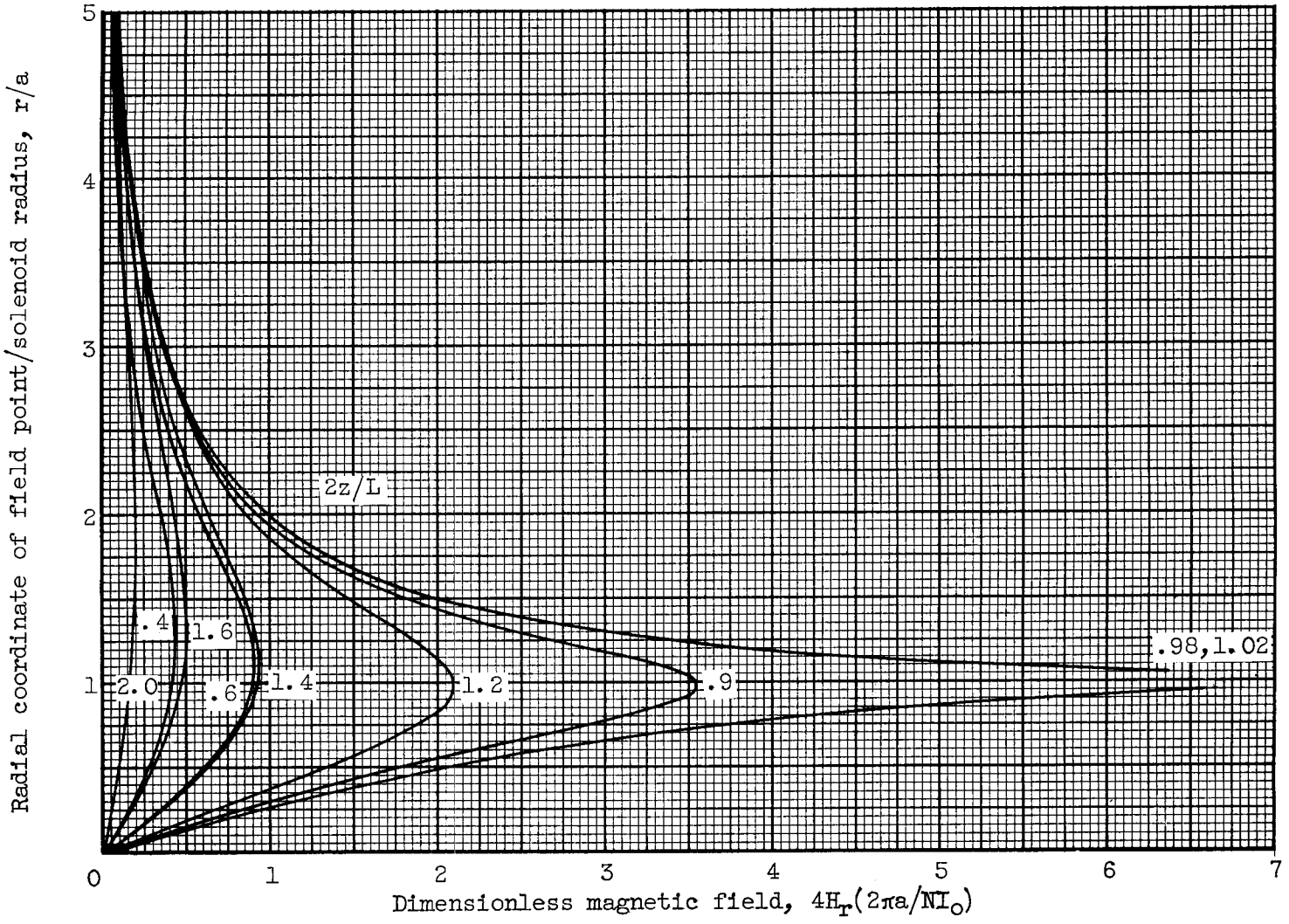

(f) Helical angle, 15.0°; length-radius ratio, 5.0.

Figure 2. - Continued. Dimensionless radial field of helical solenoid.

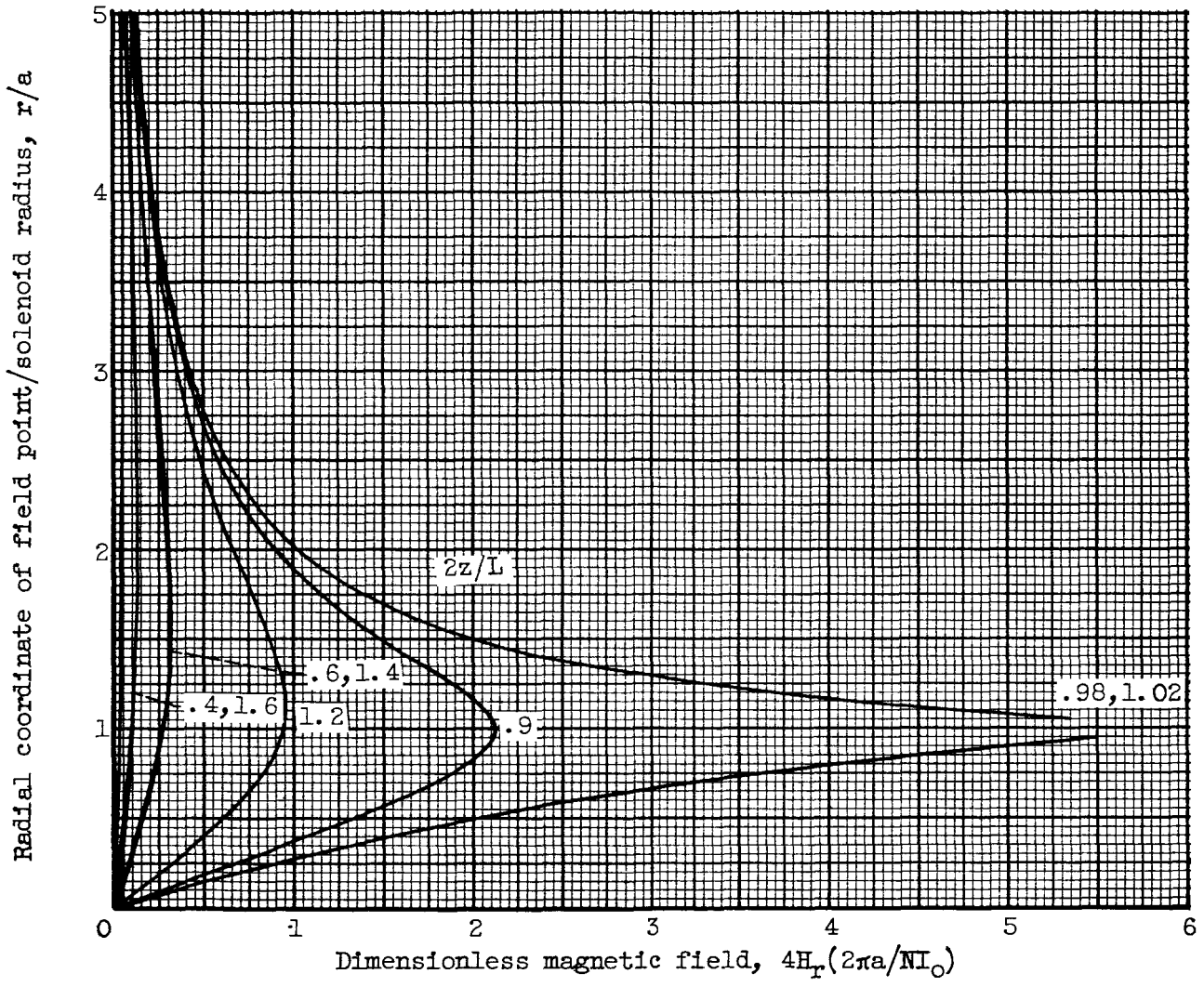

(g) Helical angle, 15.0°; length-radius ratio, 10.0.

Figure 2. - Continued. Dimensionless radial field of helical solenoid.

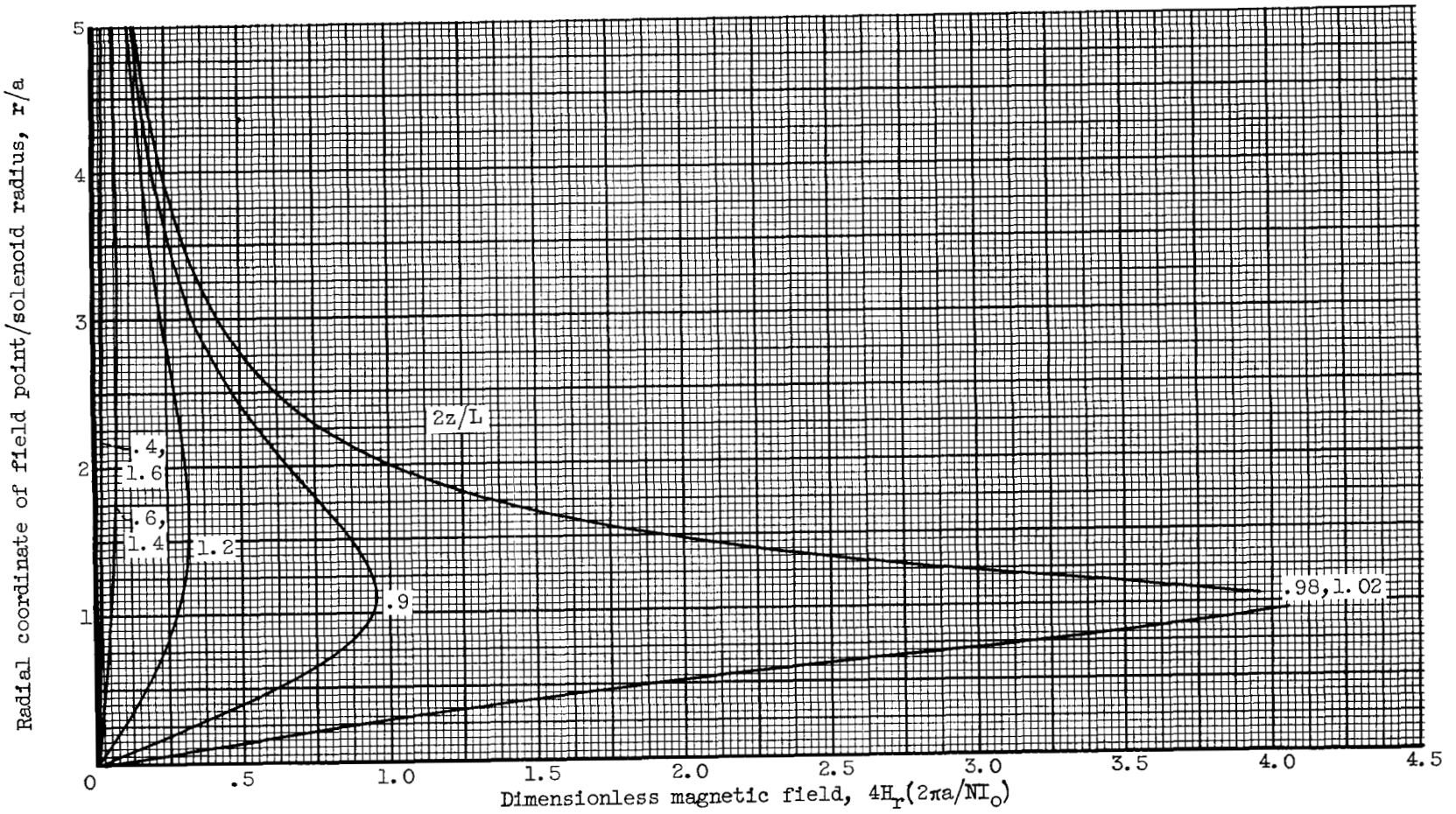

(h) Helical angle, 15.0°; length-radius ratio, 20.0.

Figure 2. - Continued. Dimensionless radial field of helical solenoid.

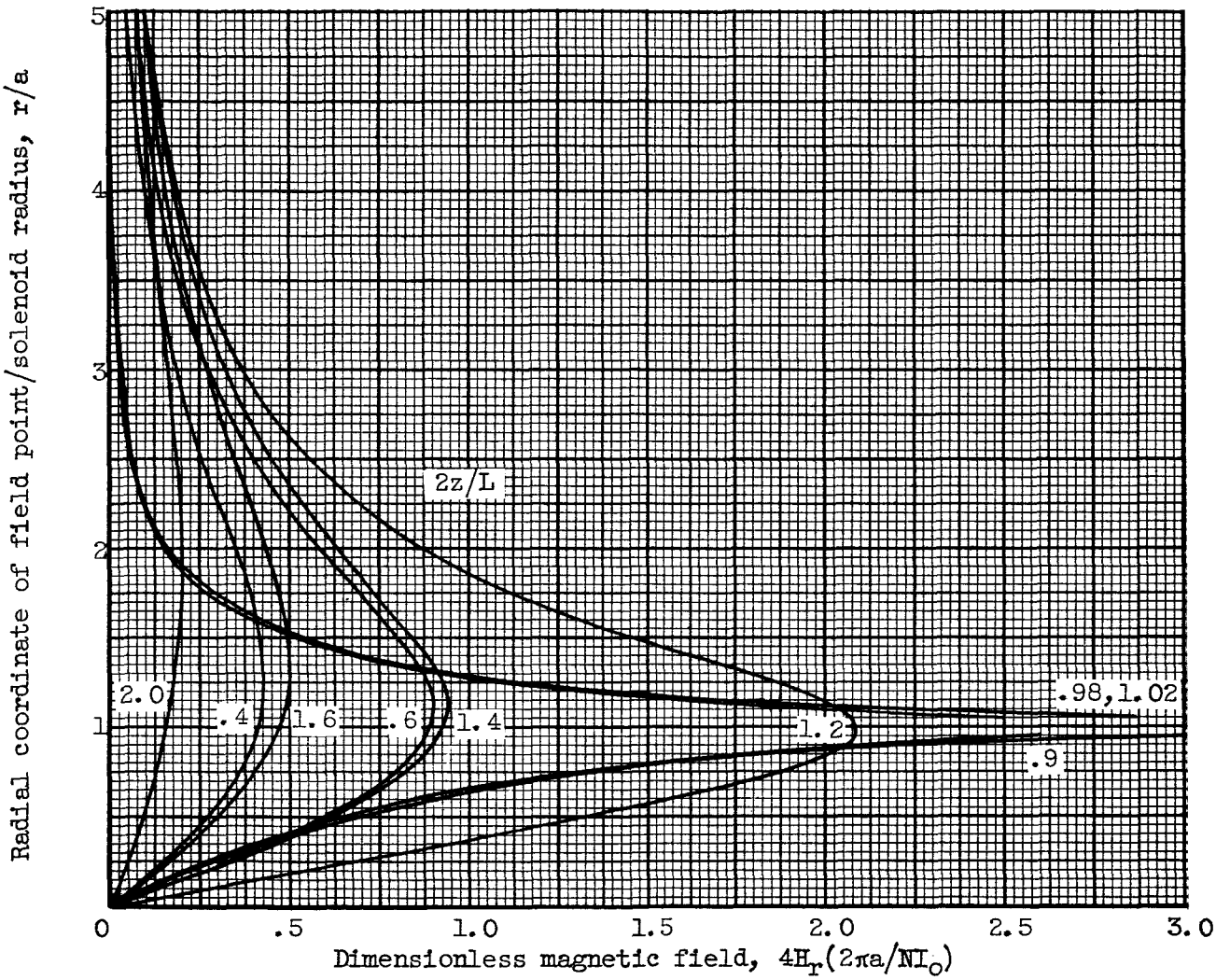

(i) Helical angle, 30.0°; length-radius ratio, 1.0.

Figure 2. - Continued. Dimensionless radial field of helical solenoid.

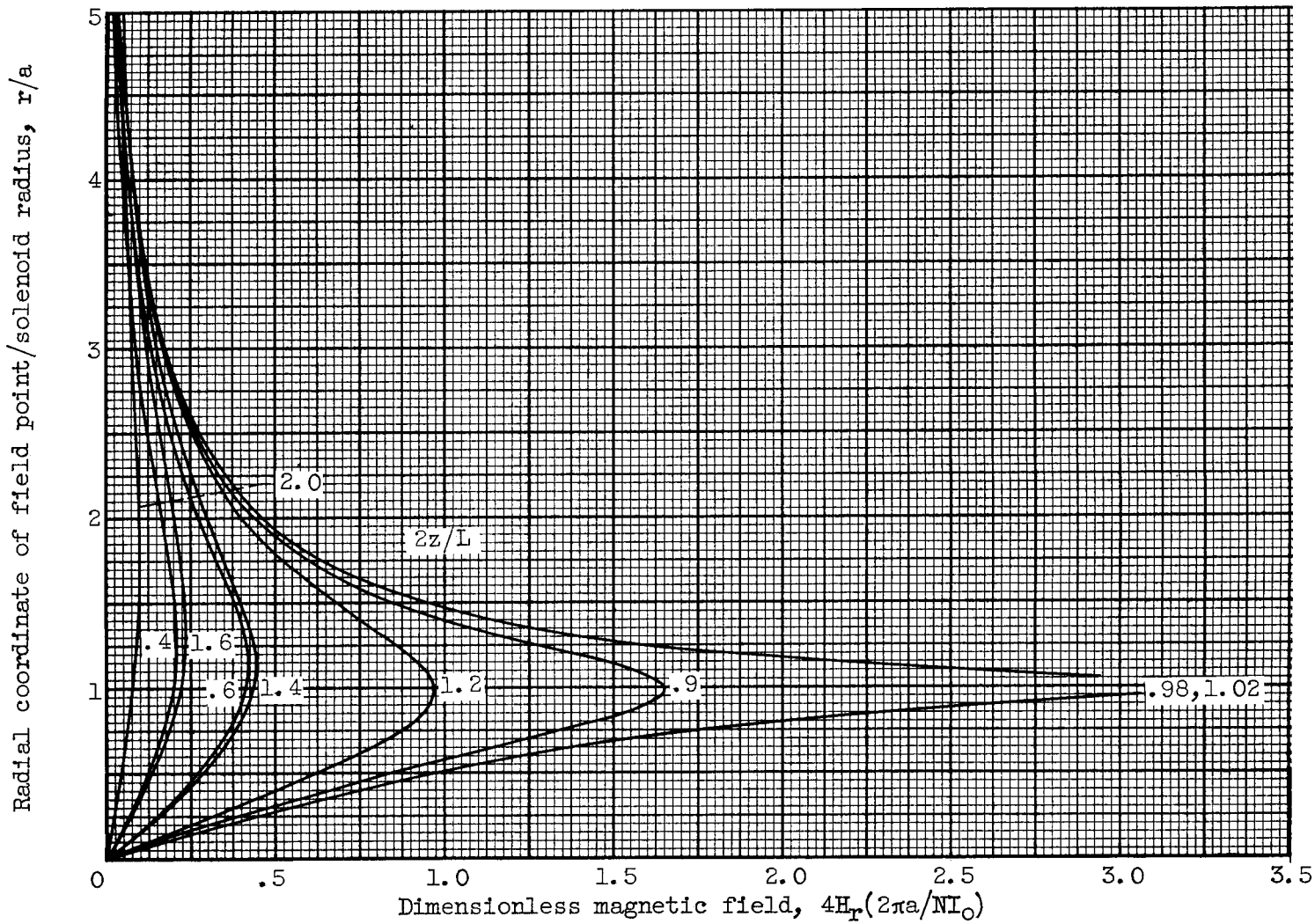

(j) Helical angle, 30.0°; length-radius ratio, 5.0.

Figure 2. - Continued. Dimensionless radial field of helical solenoid.

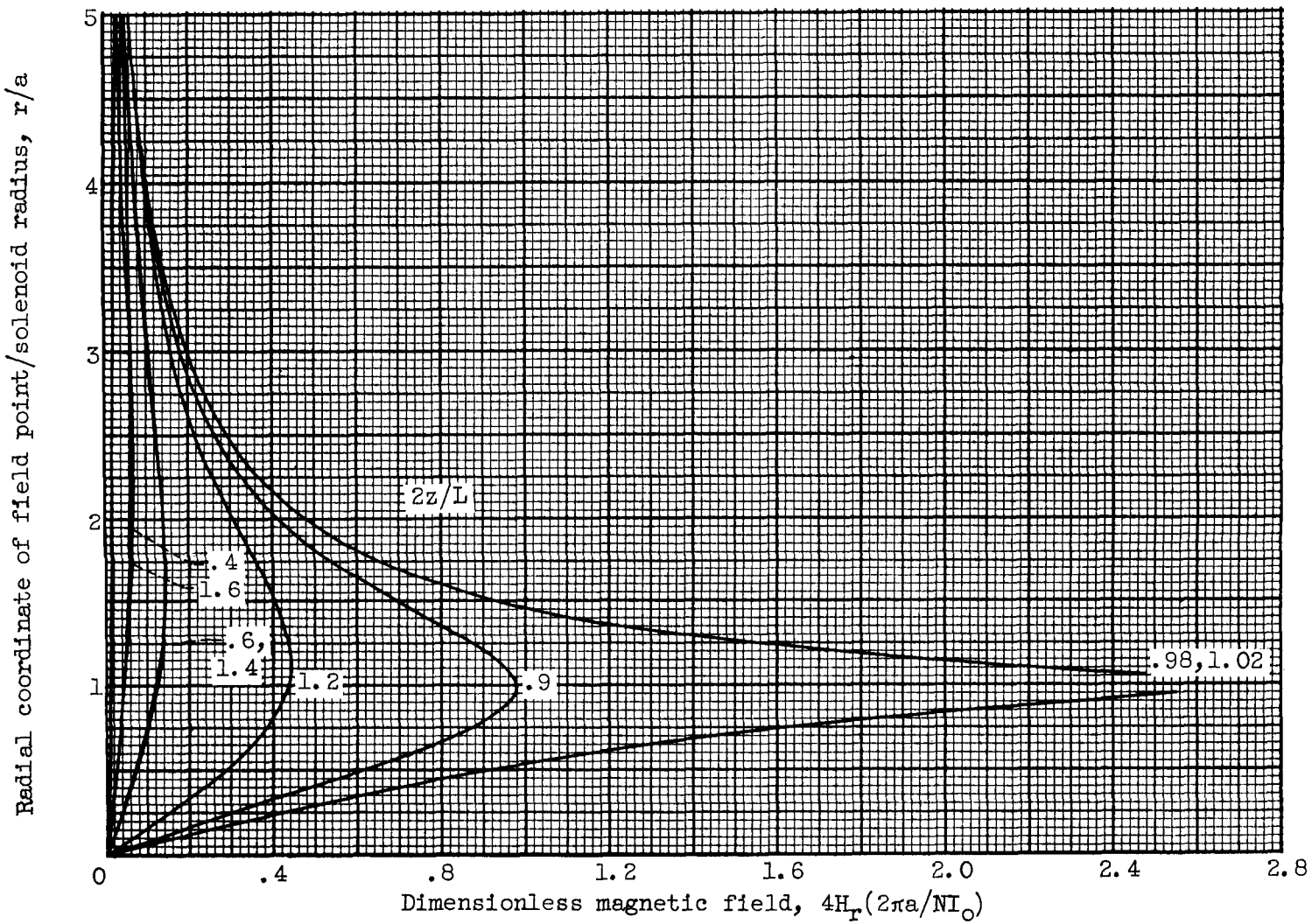

(k) Helical angle, 30.0°; length-radius ratio, 10.0.

Figure 2. - Continued. Dimensionless radial field of helical solenoid.

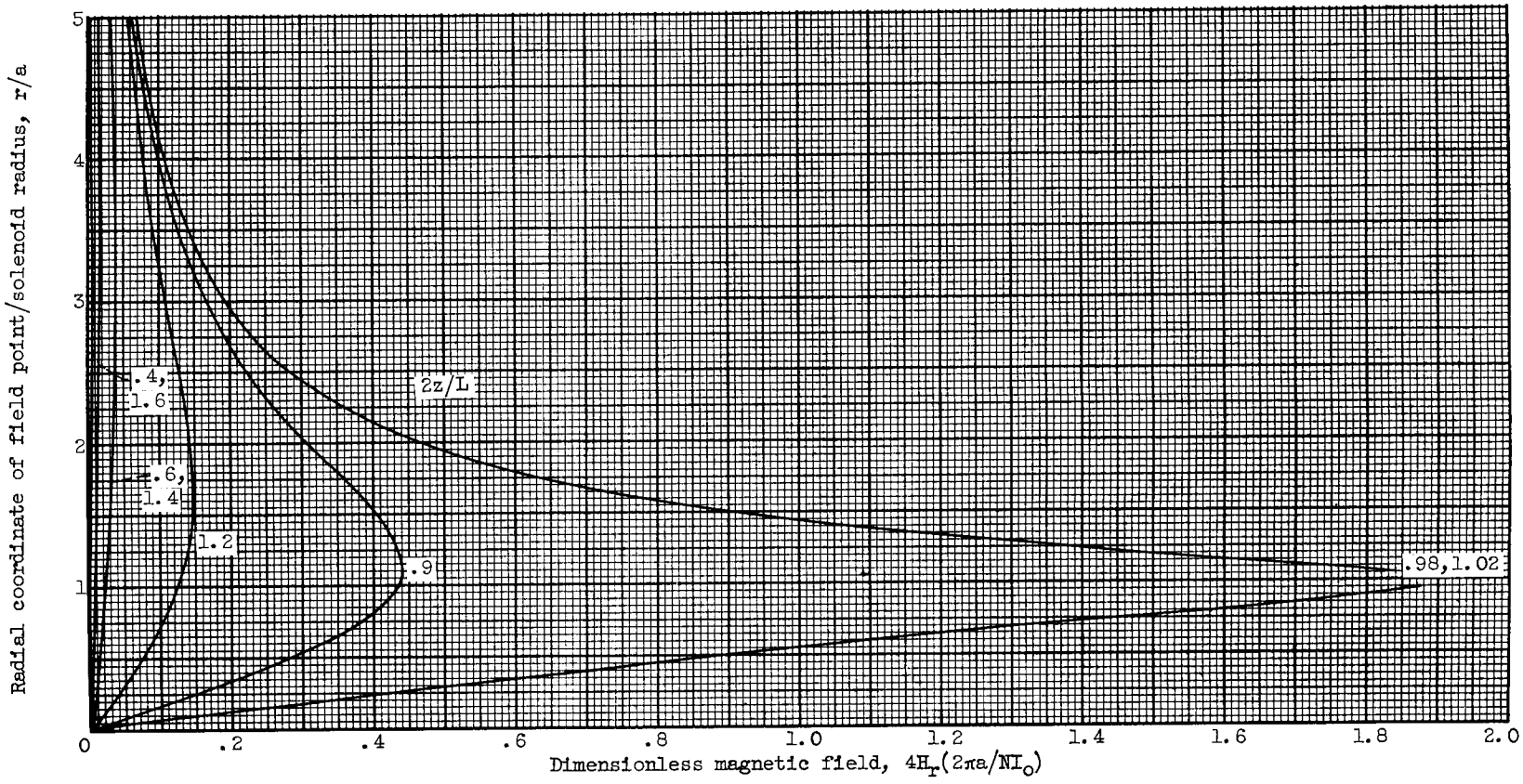

(l) Helical angle, 30.0°; length-radius ratio, 20.0.

Figure 2. - Continued. Dimensionless radial field of helical solenoid.

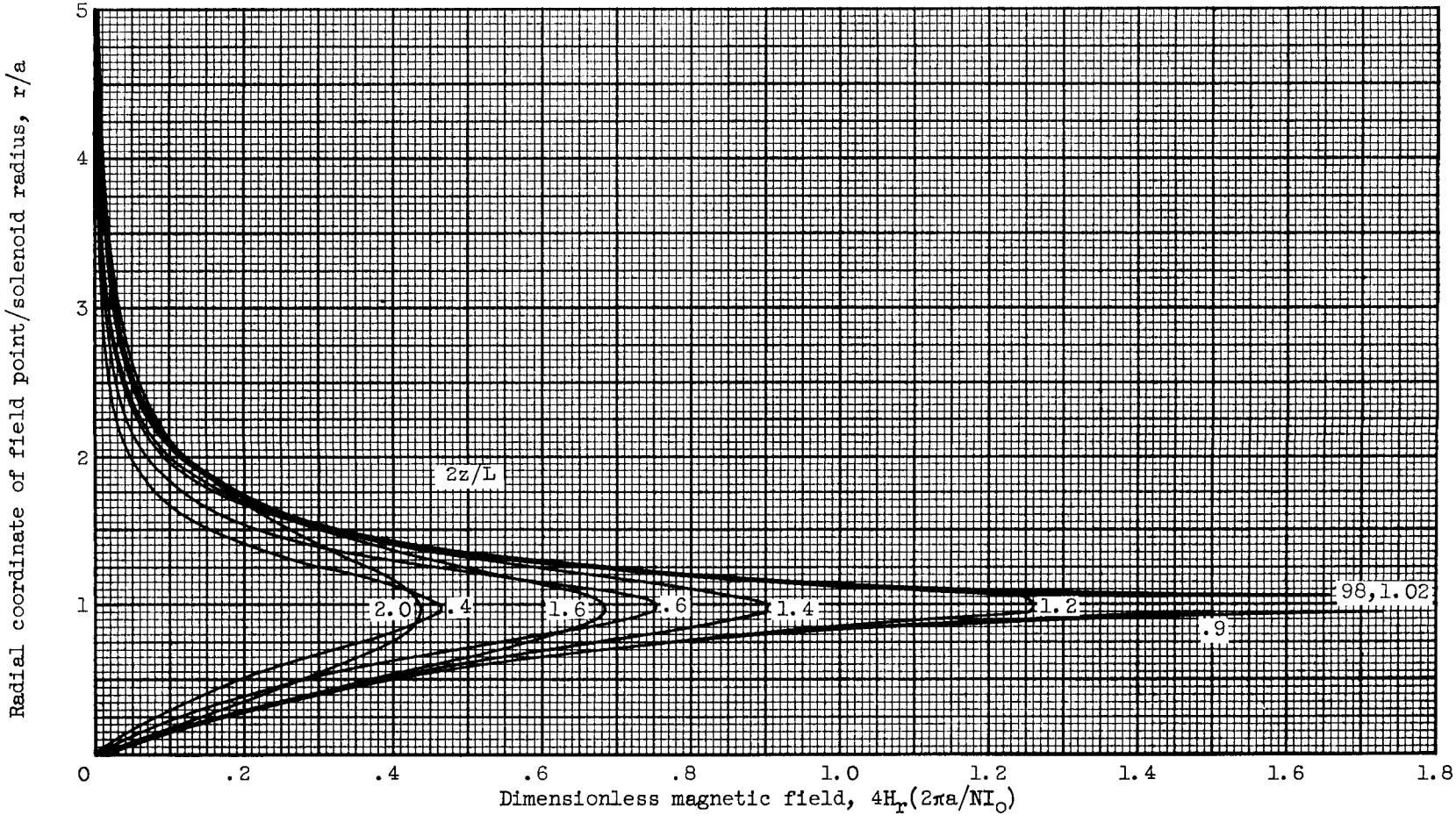

(m) Helical angle, 45.0°; length-radius ratio, 1.0.

Figure 2. - Continued. Dimensionless radial field of helical solenoid.

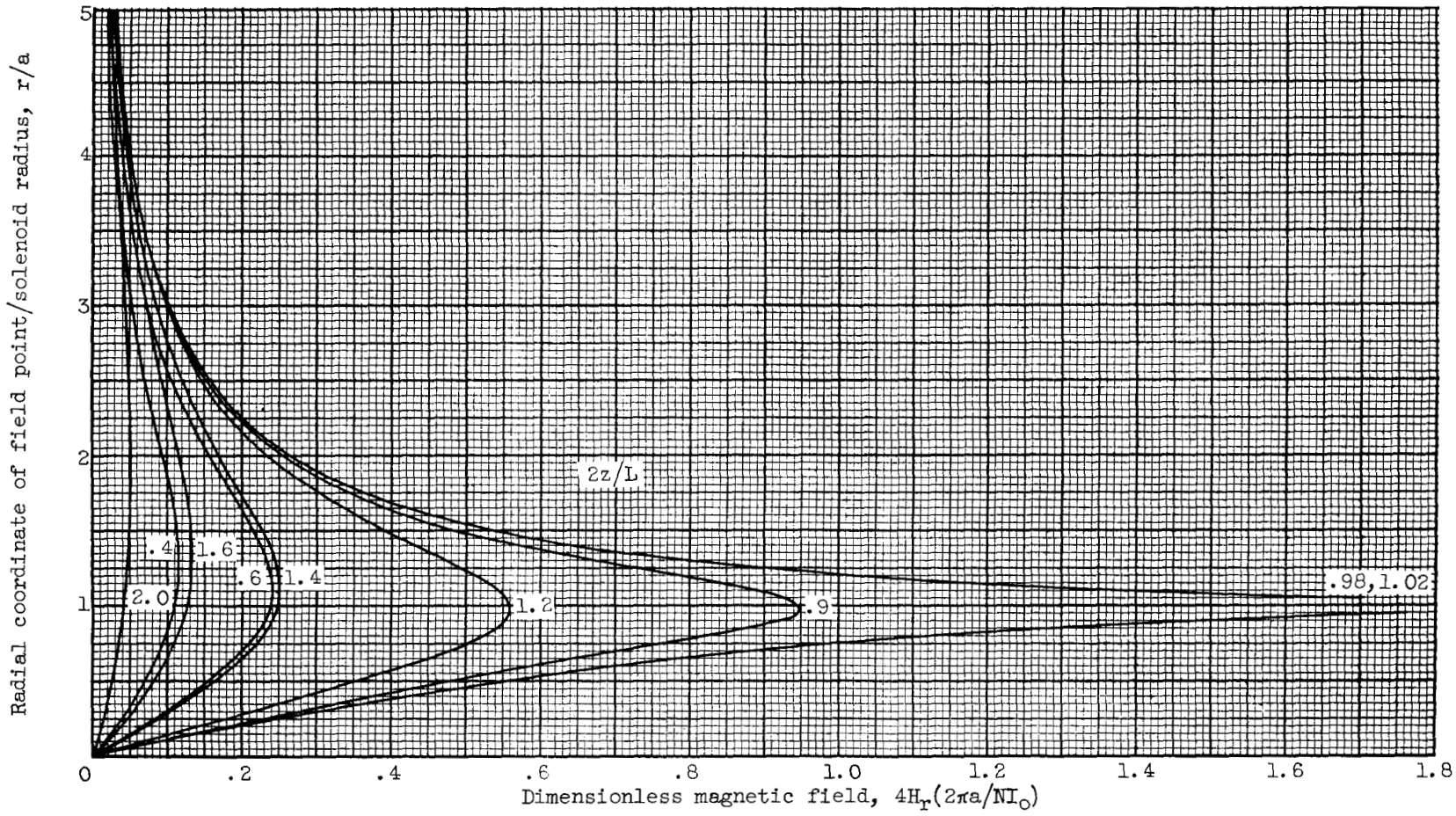

(n) Helical angle, 45.0°; length-radius ratio, 5.0.

Figure 2. - Continued. Dimensionless radial field of helical solenoid.

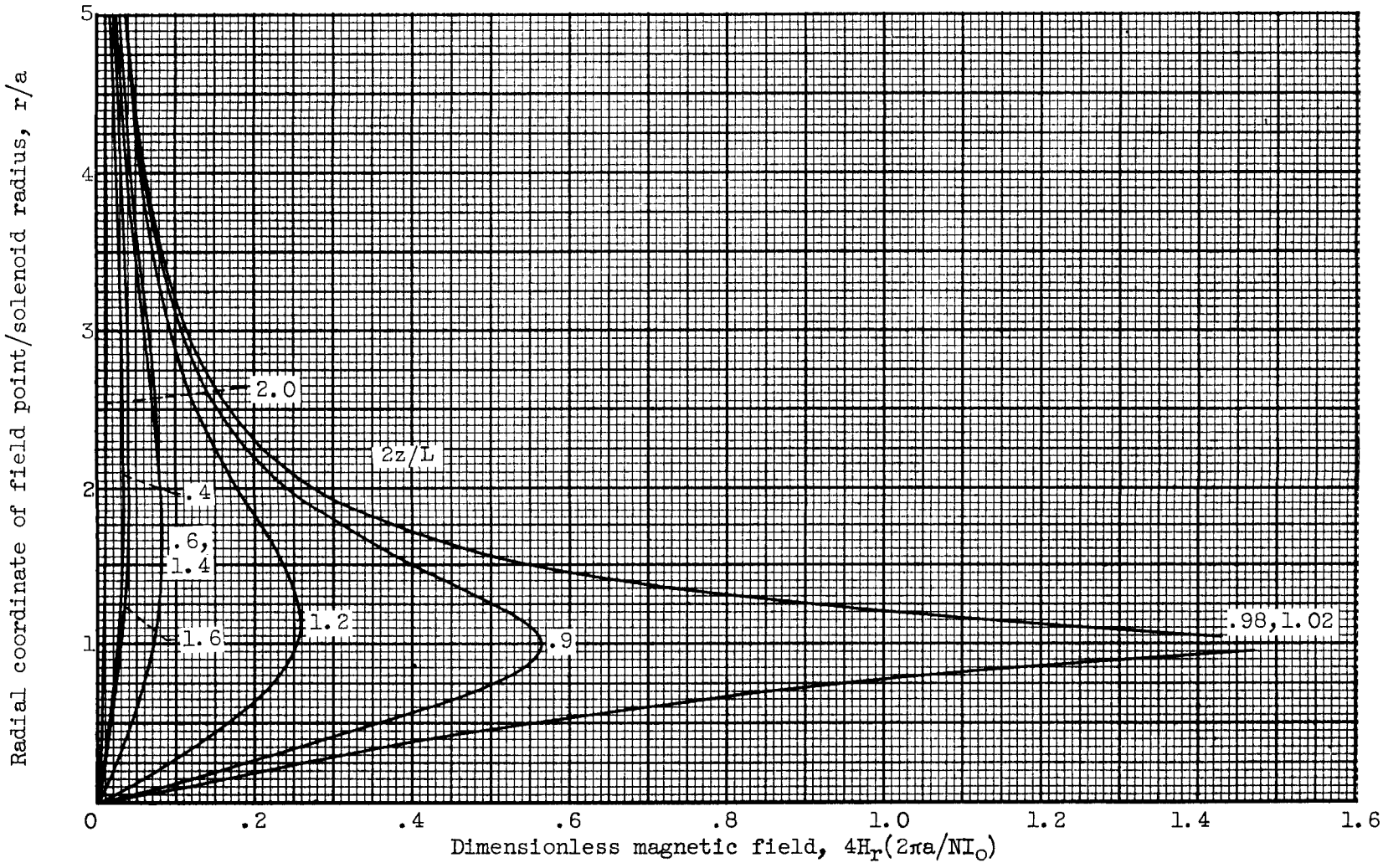

(o) Helical angle, 45.0°; length-radius ratio, 10.0.

Figure 2. - Continued. Dimensionless radial field of helical solenoid.

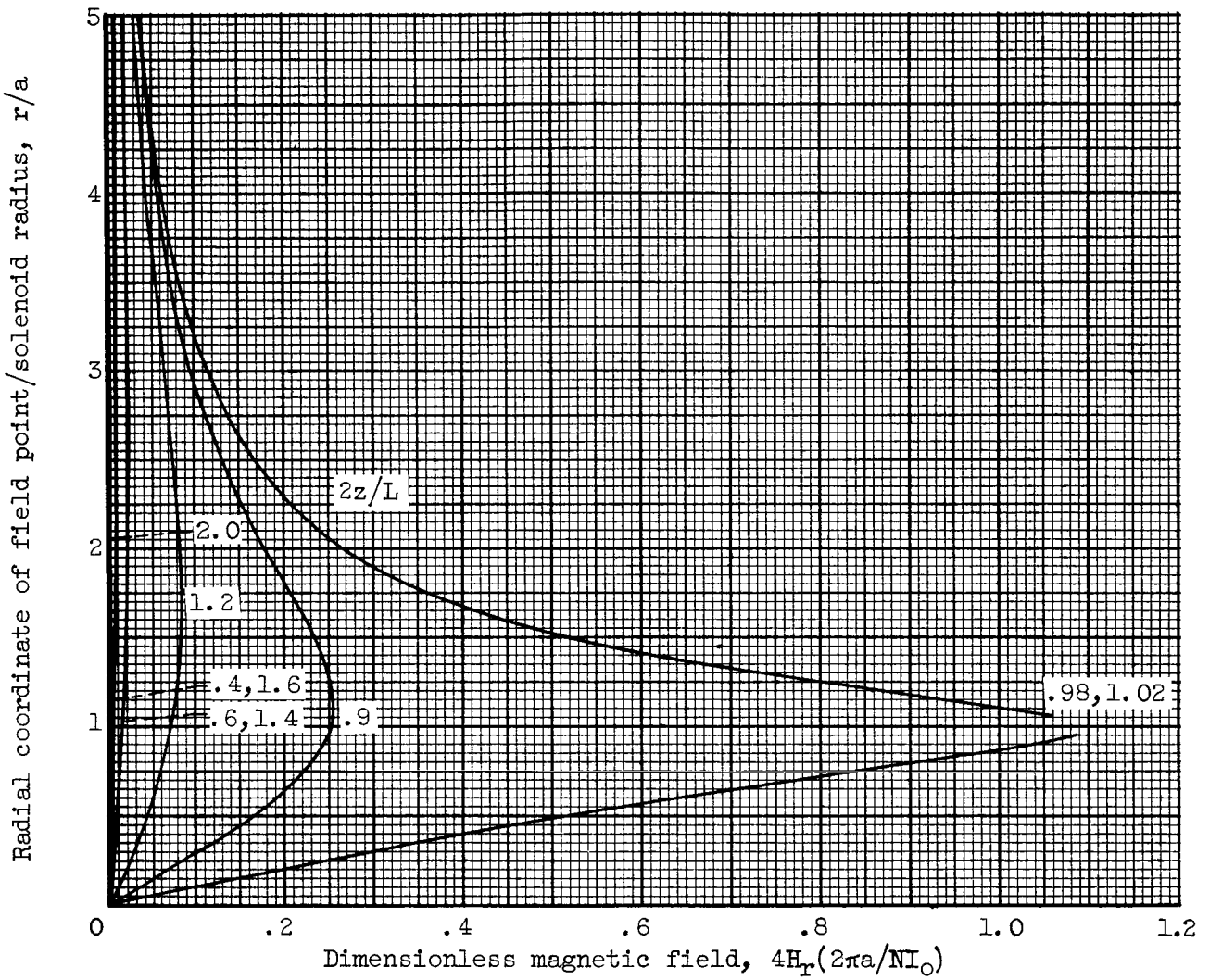

(p) Helical angle, 45.0°; length-radius ratio, 20.0.

Figure 2. - Concluded. Dimensionless radial field of helical solenoid.

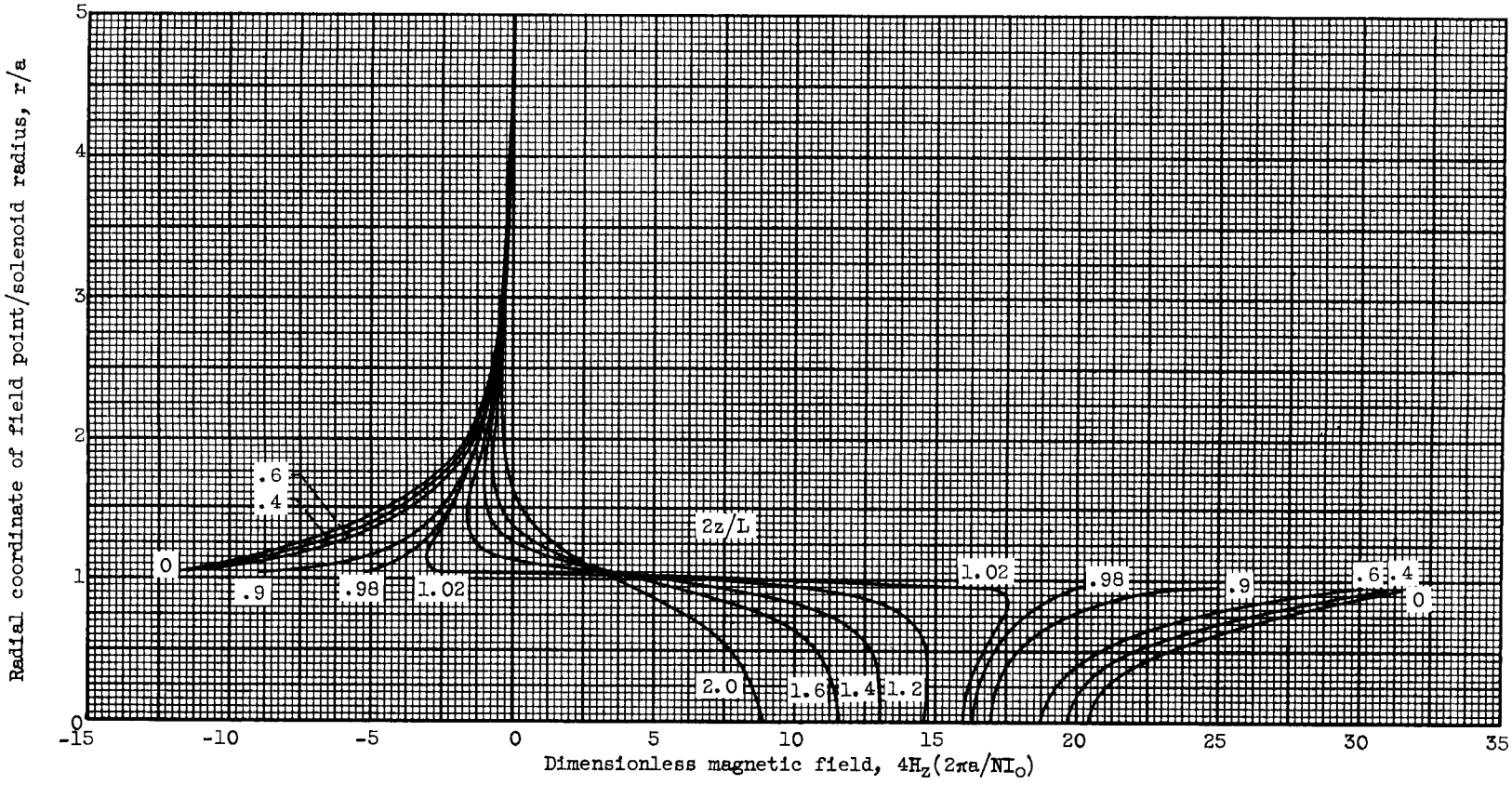

(a) Helical angle, 5.0°; length-radius ratio, 1.0.

Figure 3. - Dimensionless axial field of helical solenoid.

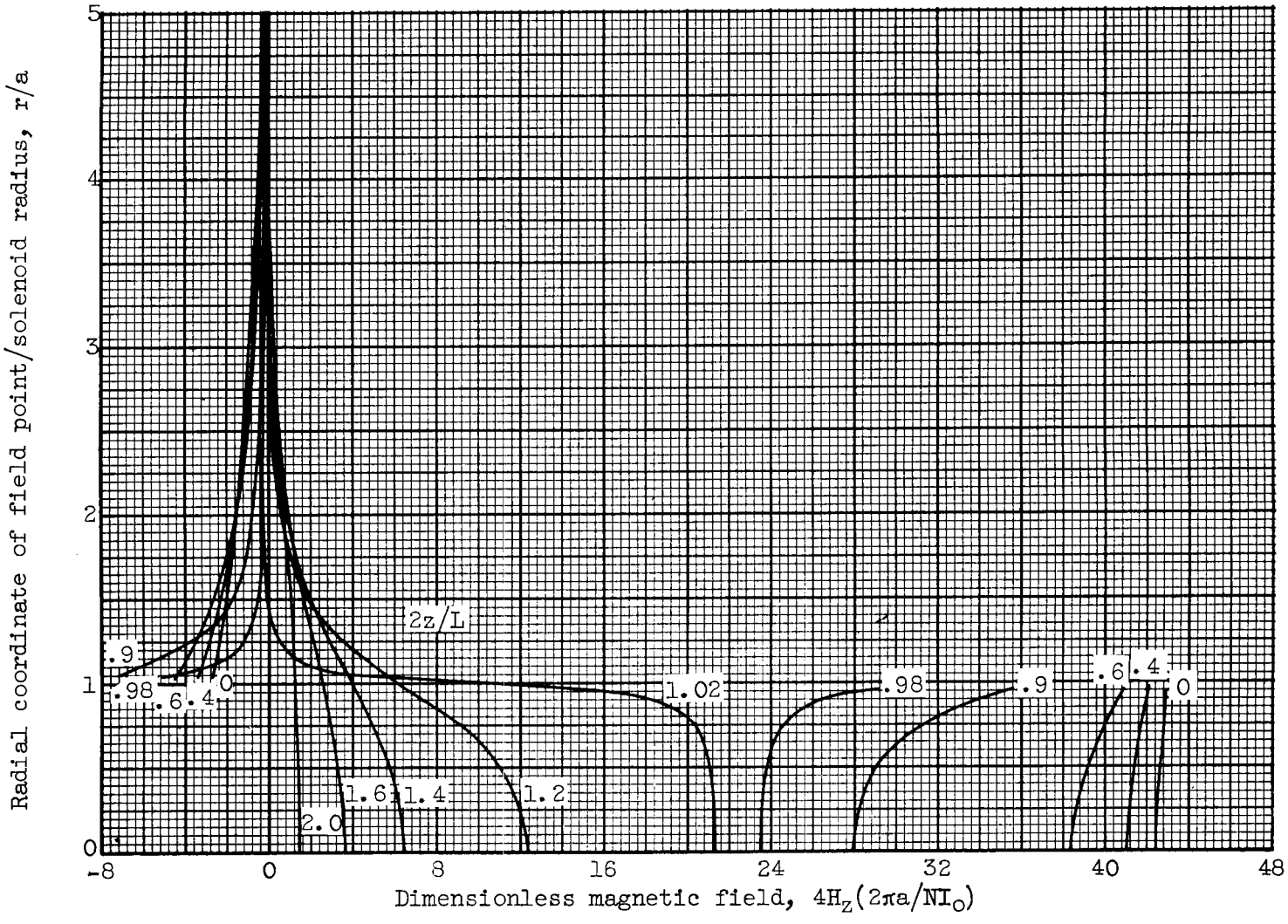

(b) Helical angle, 5.0°; length-radius ratio, 5.0.

Figure 3. - Continued. Dimensionless axial field of helical solenoid.

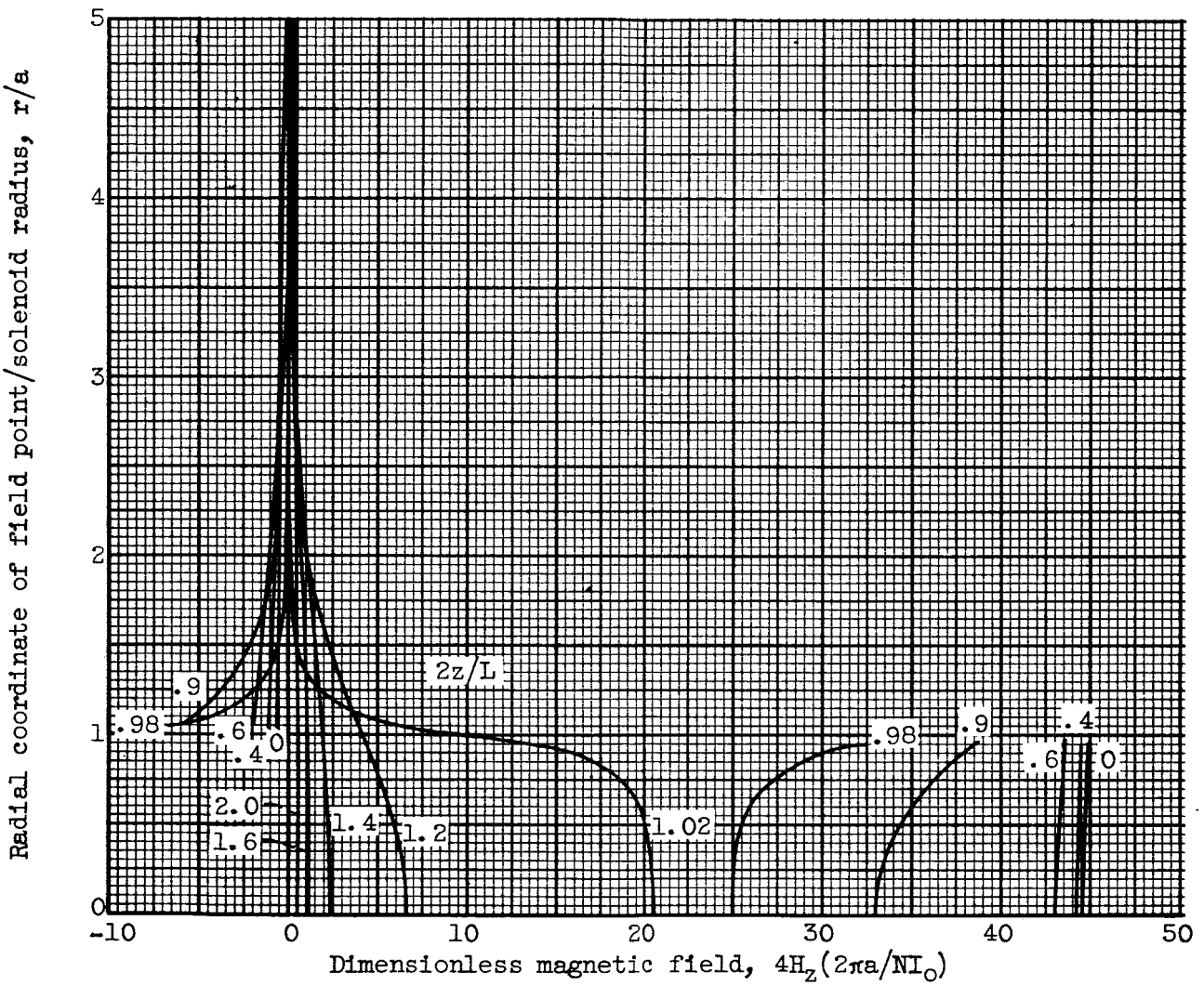

(c) Helical angle, 5.0°; length-radius ratio, 10.0.

Figure 3. - Continued. Dimensionless axial field of helical solenoid.

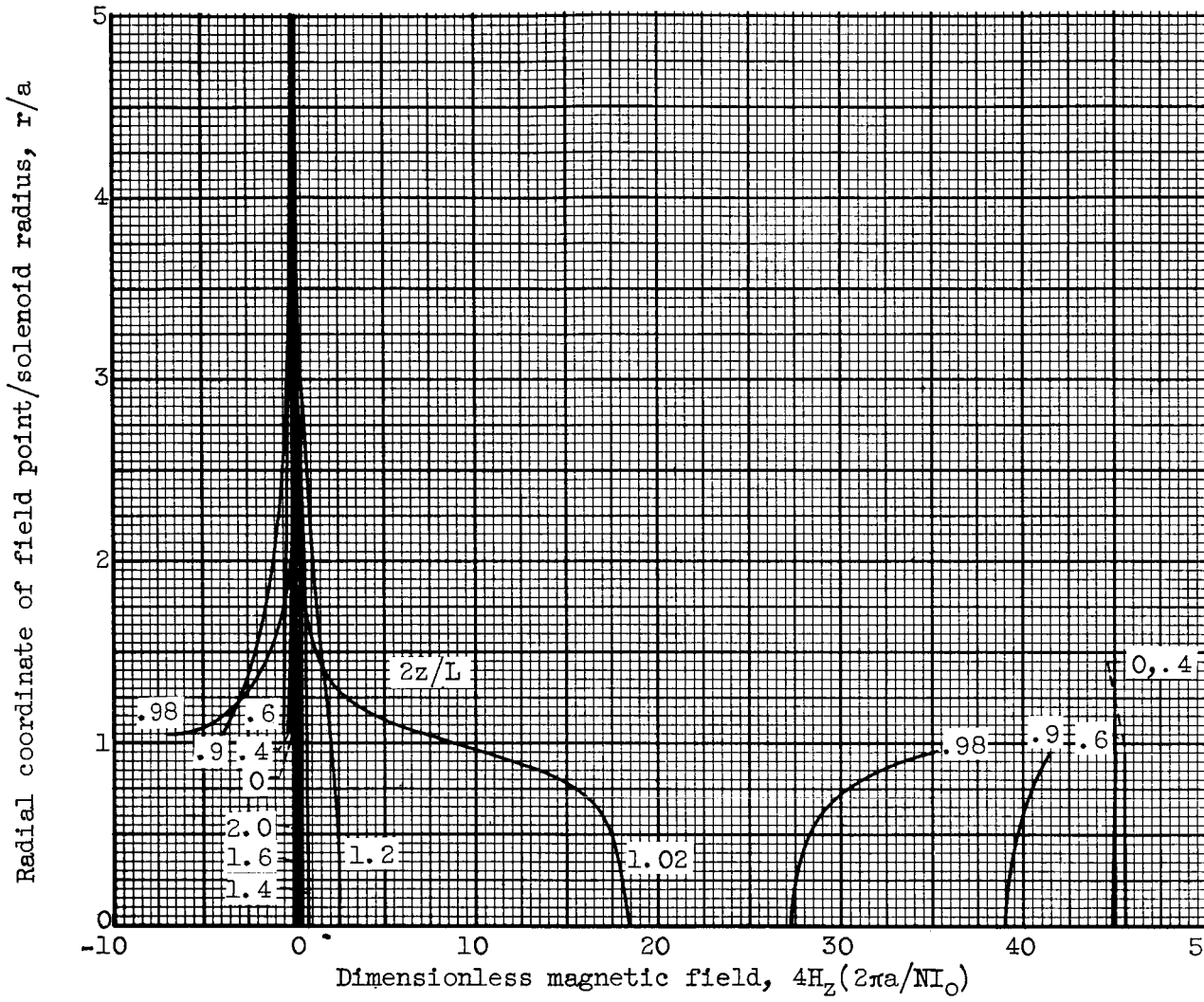

(d) Helical angle, 5.0°; length-radius ratio, 20.0.

Figure 3. - Continued. Dimensionless axial field of helical solenoid.

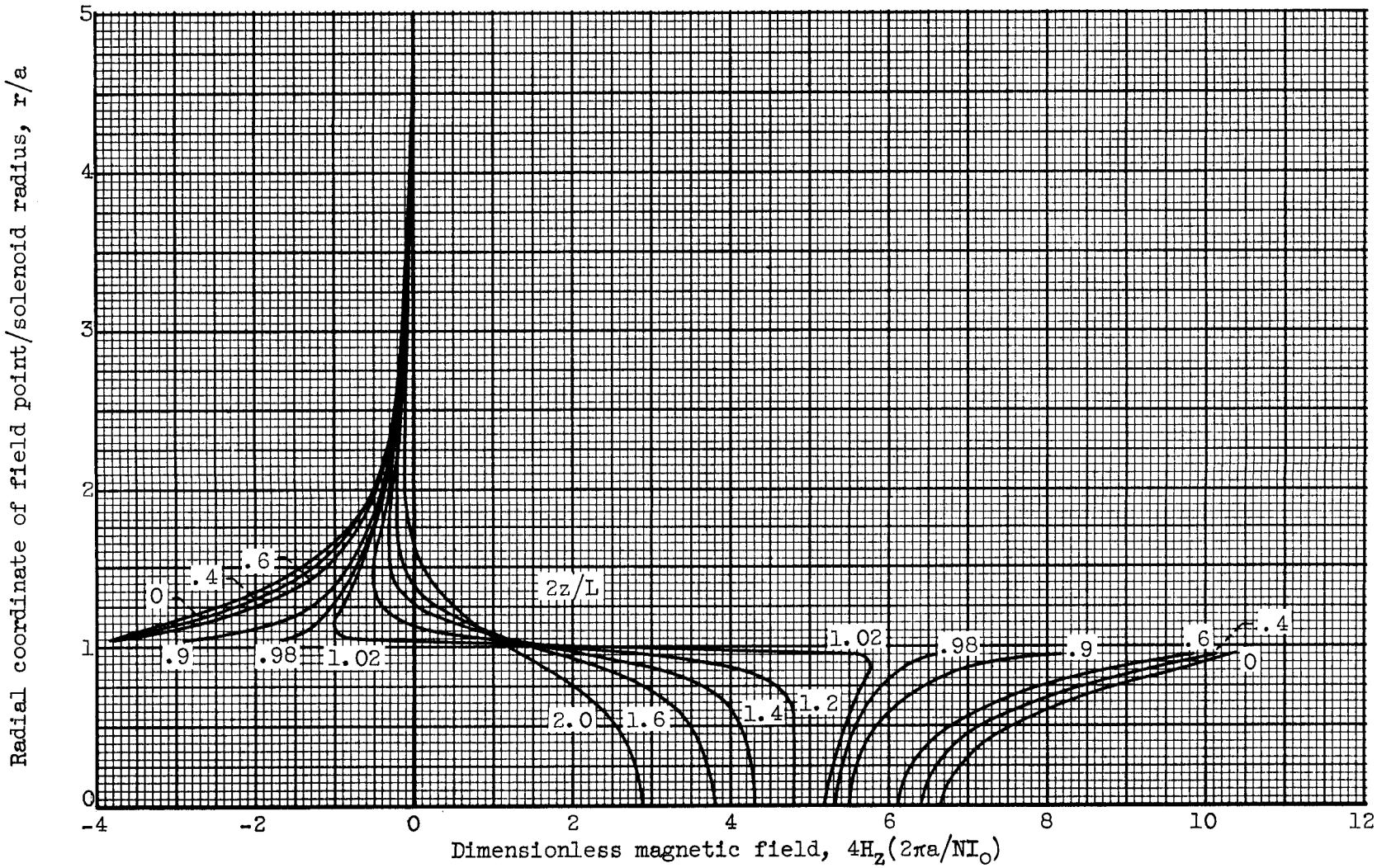

(e) Helical angle, 15.0°; length-radius ratio, 1.0.

Figure 3. - Continued. Dimensionless axial field of helical solenoid.

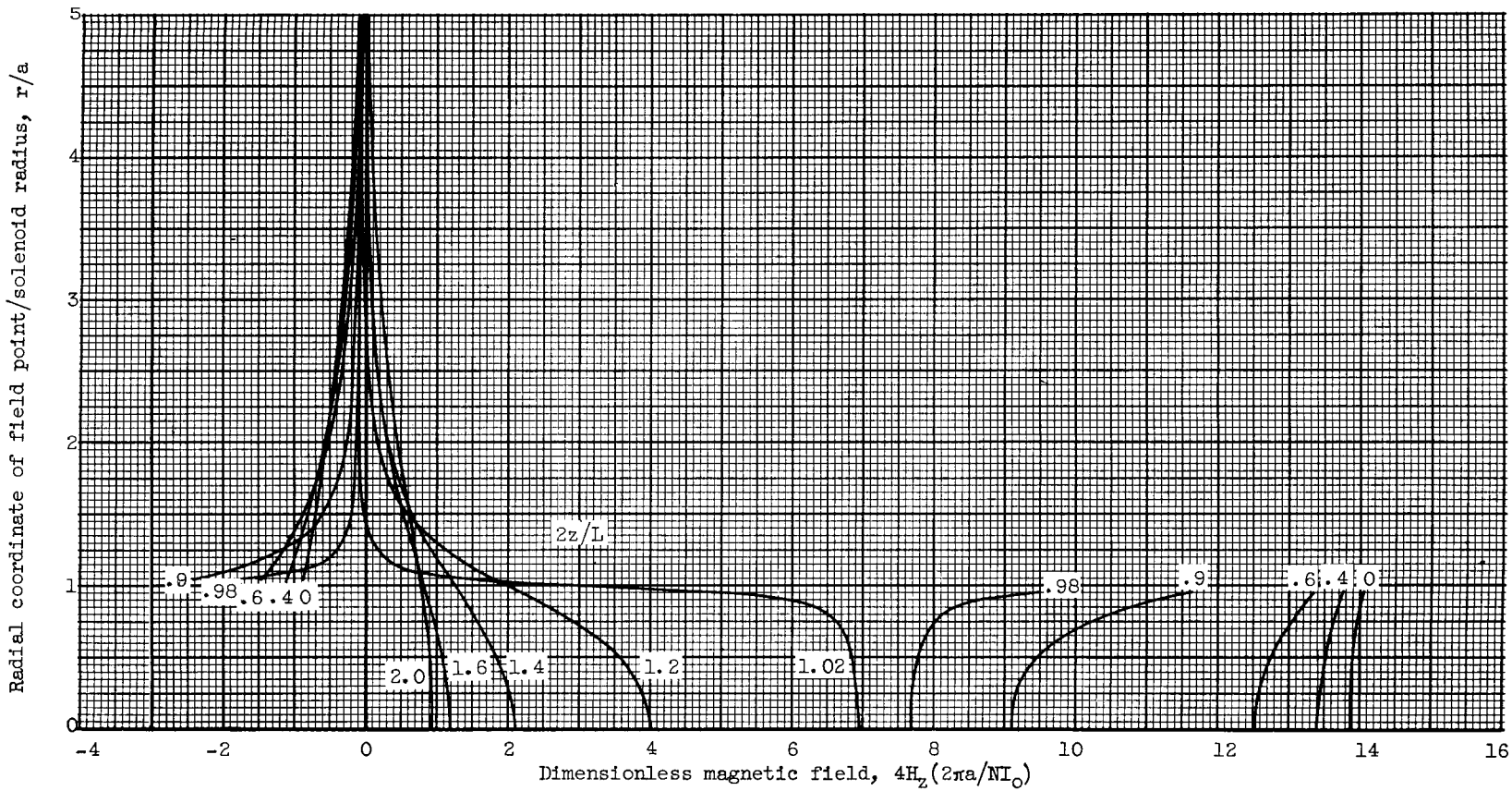

(f) Helical angle, 15.0°; length-radius ratio, 5.0.

Figure 3. - Continued. Dimensionless axial field of helical solenoid.

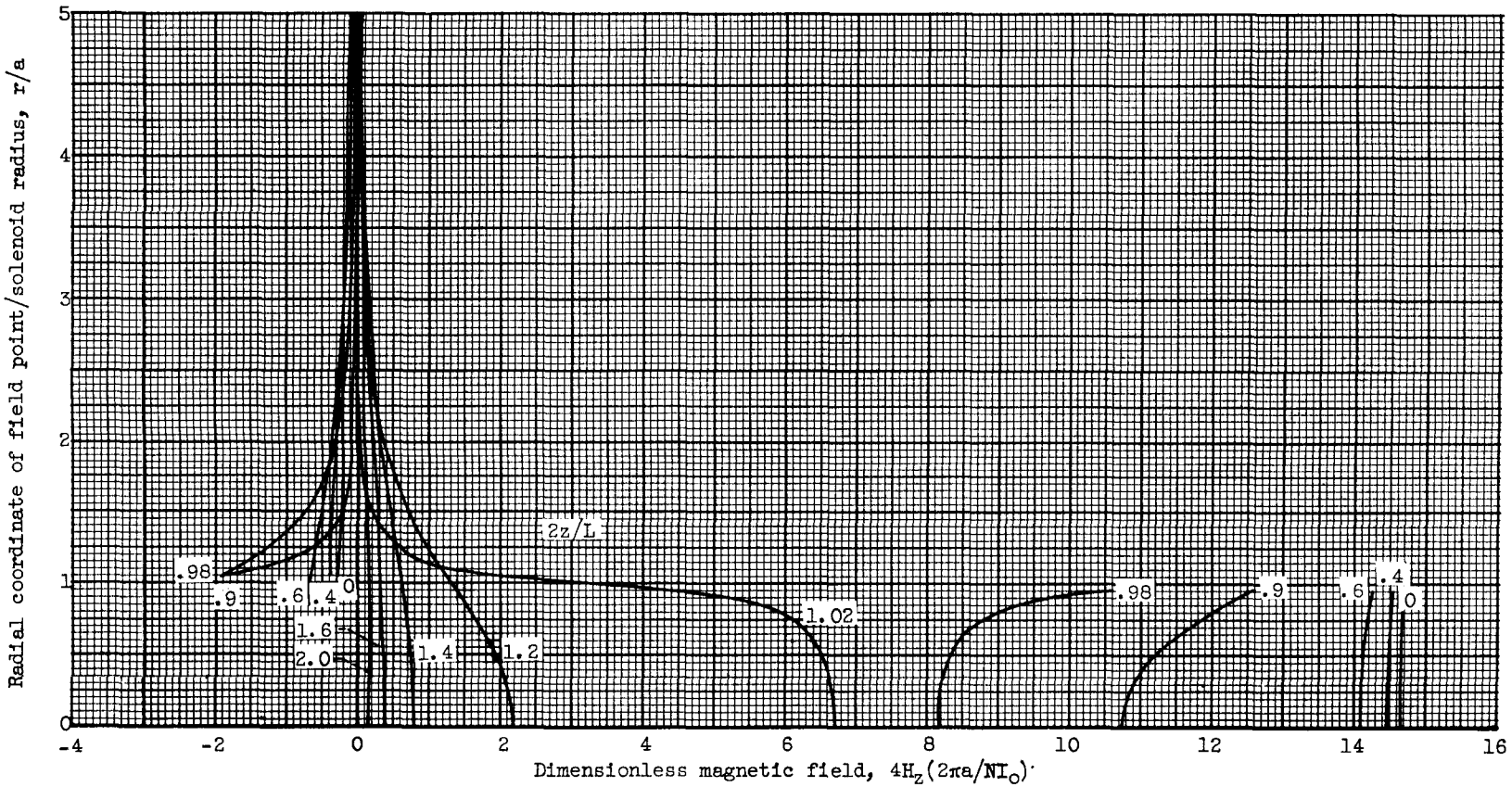

(g) Helical angle, 15.0°; length-radius ratio, 10.0.

Figure 3. - Continued. Dimensionless axial field of helical solenoid.

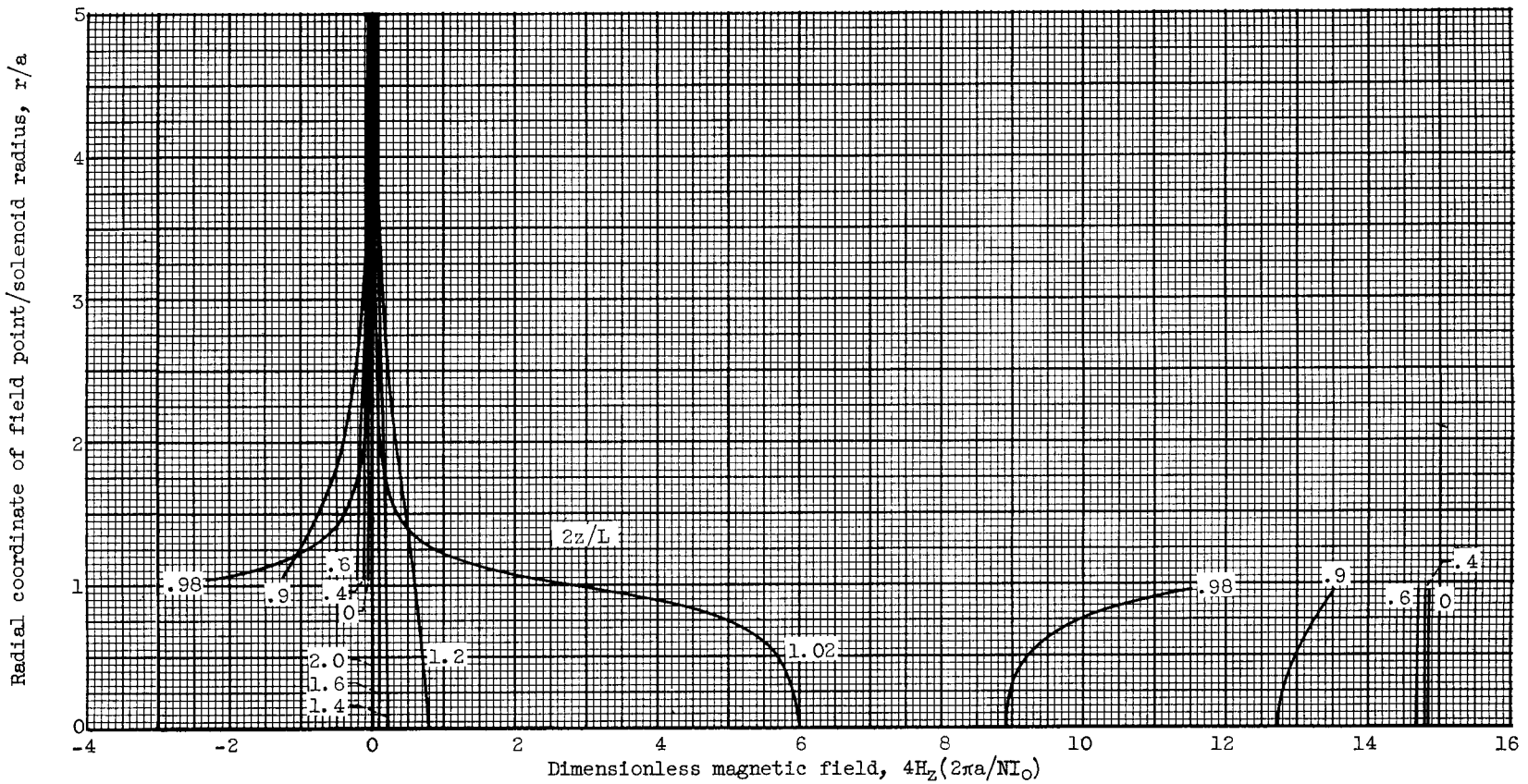

(h) Helical angle, 15.0°; length-radius ratio, 20.0.

Figure 3. - Continued. Dimensionless axial field of helical solenoid.

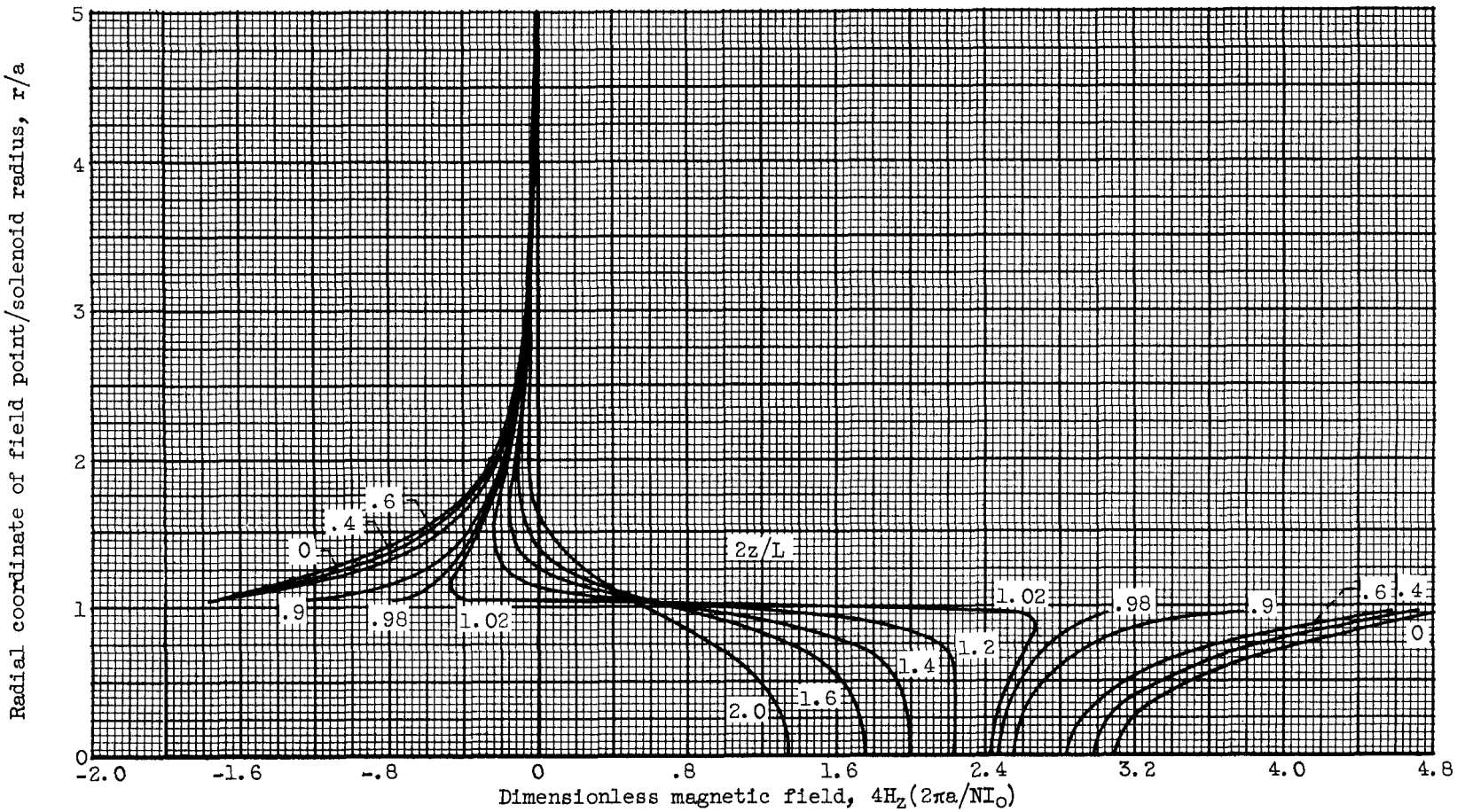

(i) Helical angle, 30.0°; length-radius ratio, 1.0.

Figure 3. - Continued. Dimensionless axial field of helical solenoid.

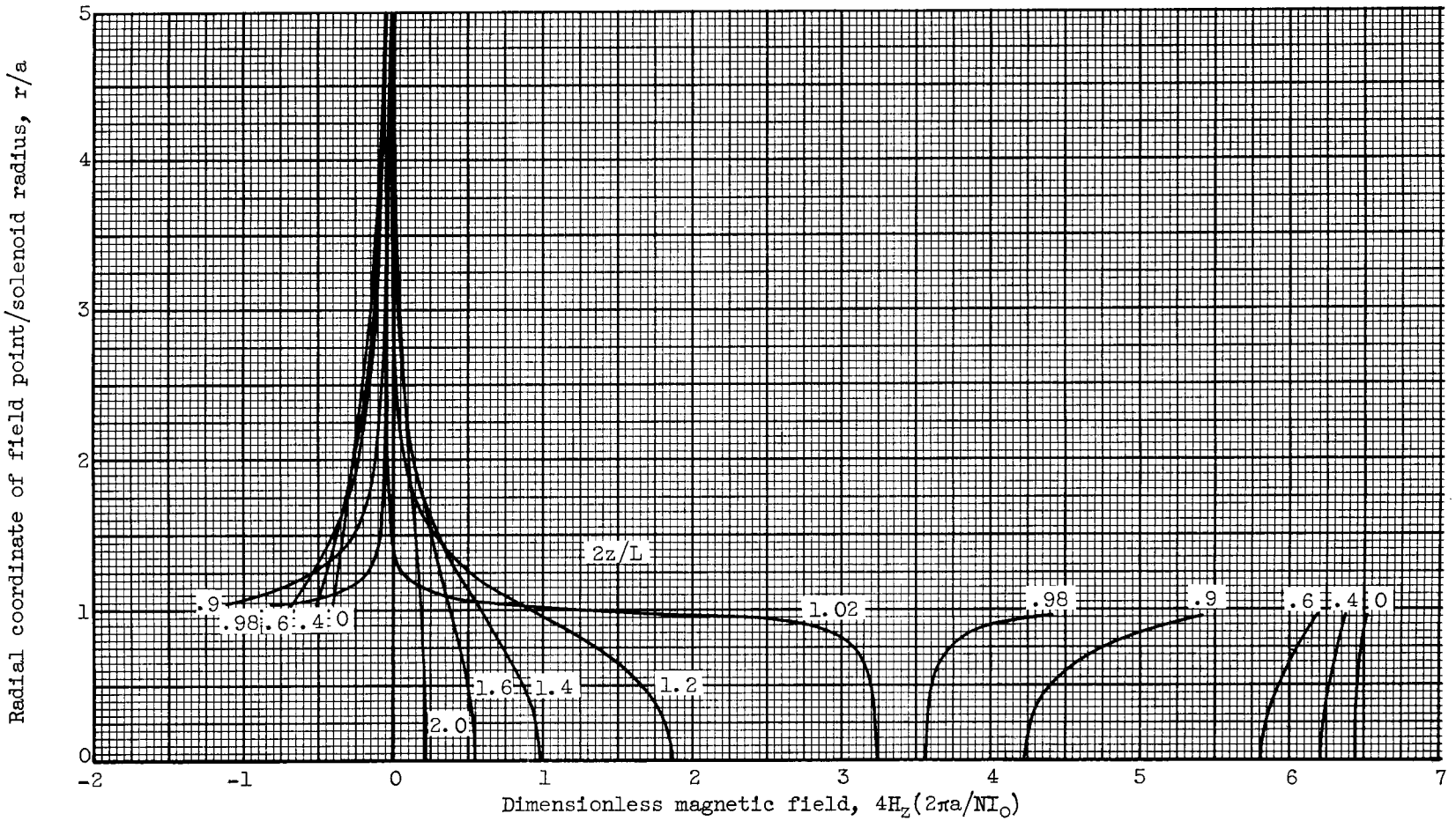

(j) Helical angle, 30.0°; length-radius ratio, 5.0.

Figure 3. - Continued. Dimensionless axial field of helical solenoid.

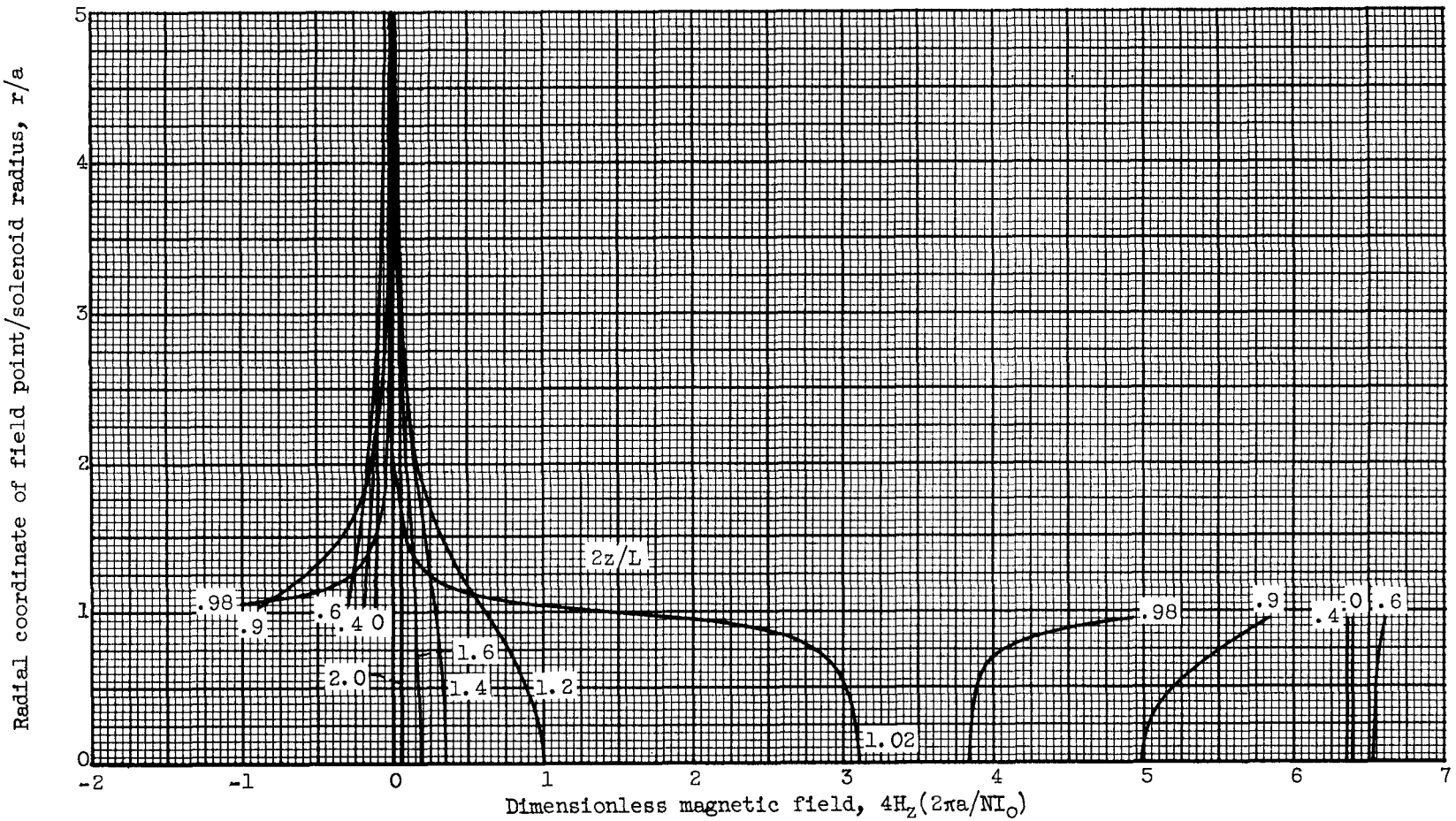

(k) Helical angle, 30.0°; length-radius ratio, 10.0.

Figure 3. - Continued. Dimensionless axial field of helical solenoid.

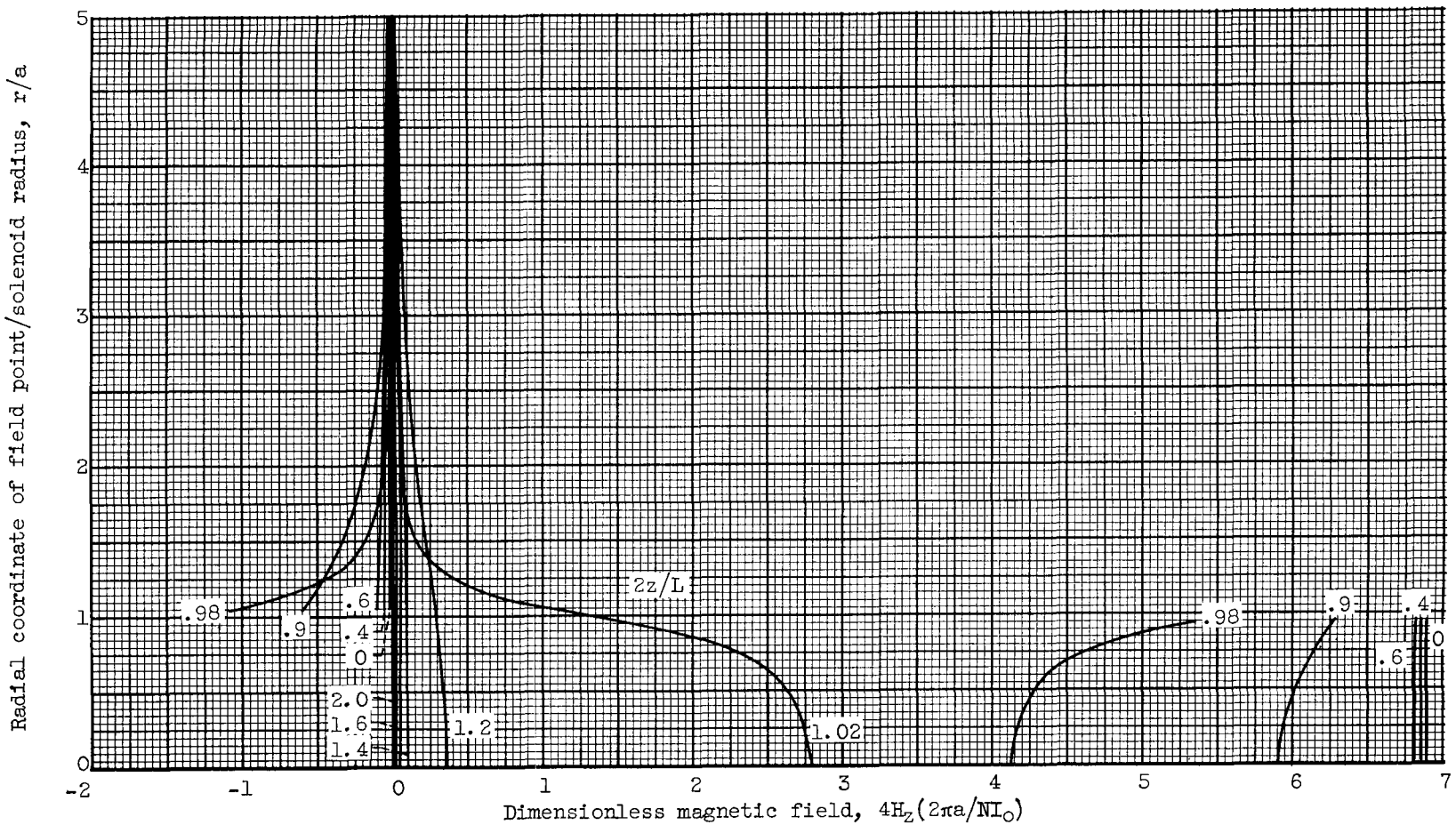

(*l*) Helical angle, 30.0°; length-radius ratio, 20.0.

Figure 3. - Continued. Dimensionless axial field of helical solenoid.

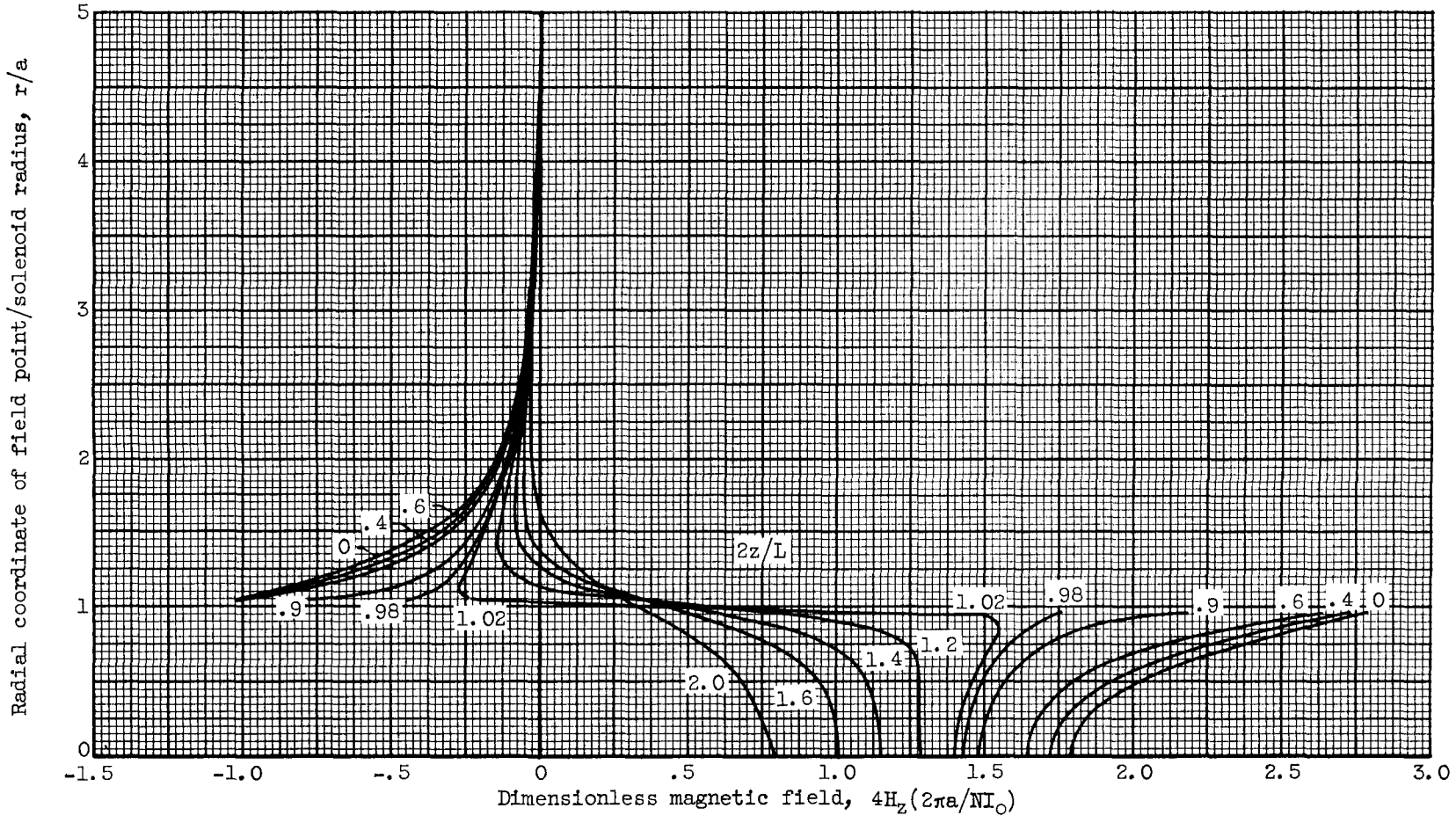

(m) Helical angle, 45.0°; length-radius ratio, 1.0.

Figure 3. - Continued. Dimensionless axial field of helical solenoid.

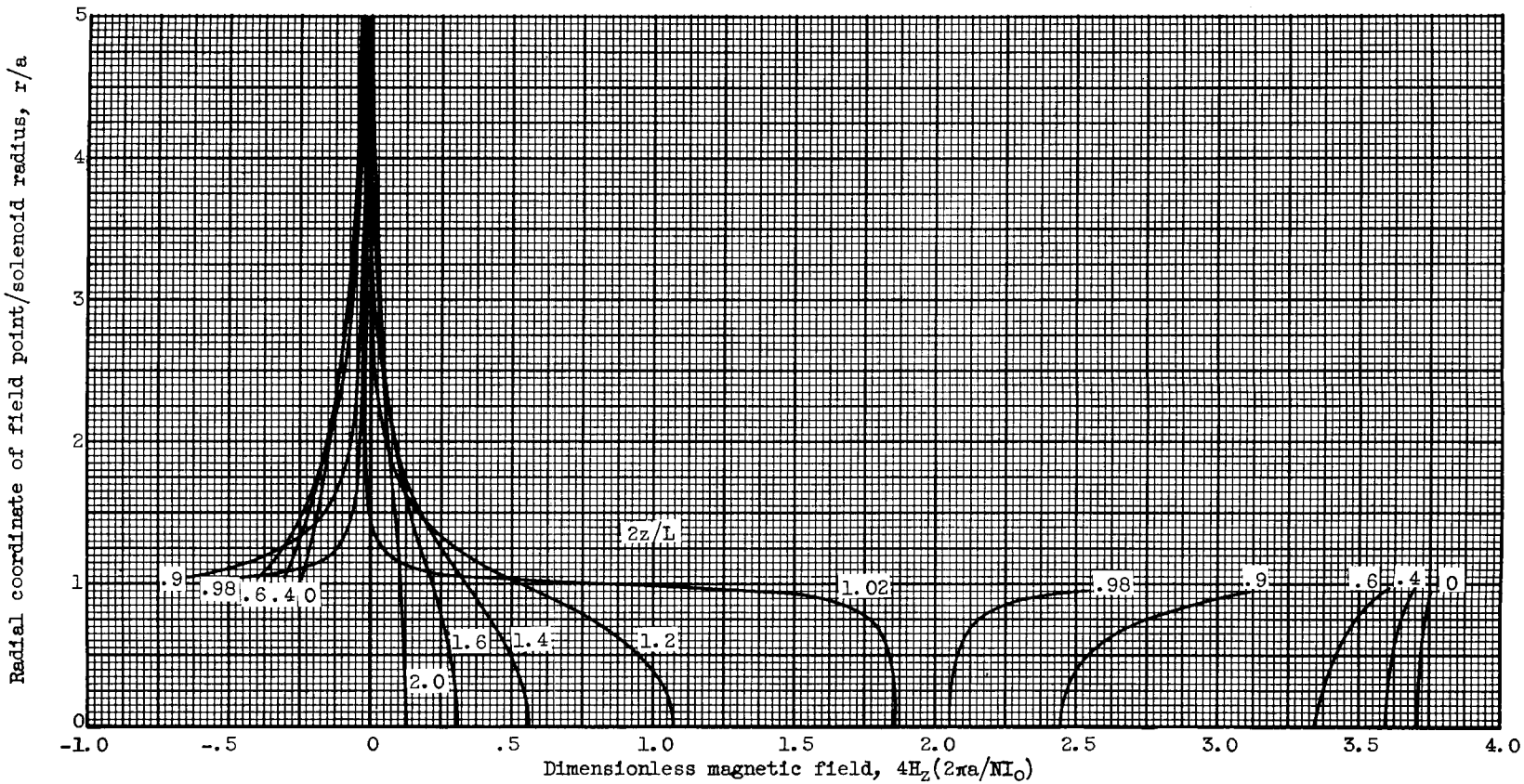

(n) Helical angle, 45.0°; length-radius ratio, 5.0.

Figure 3. - Continued. Dimensionless axial field of helical solenoid.

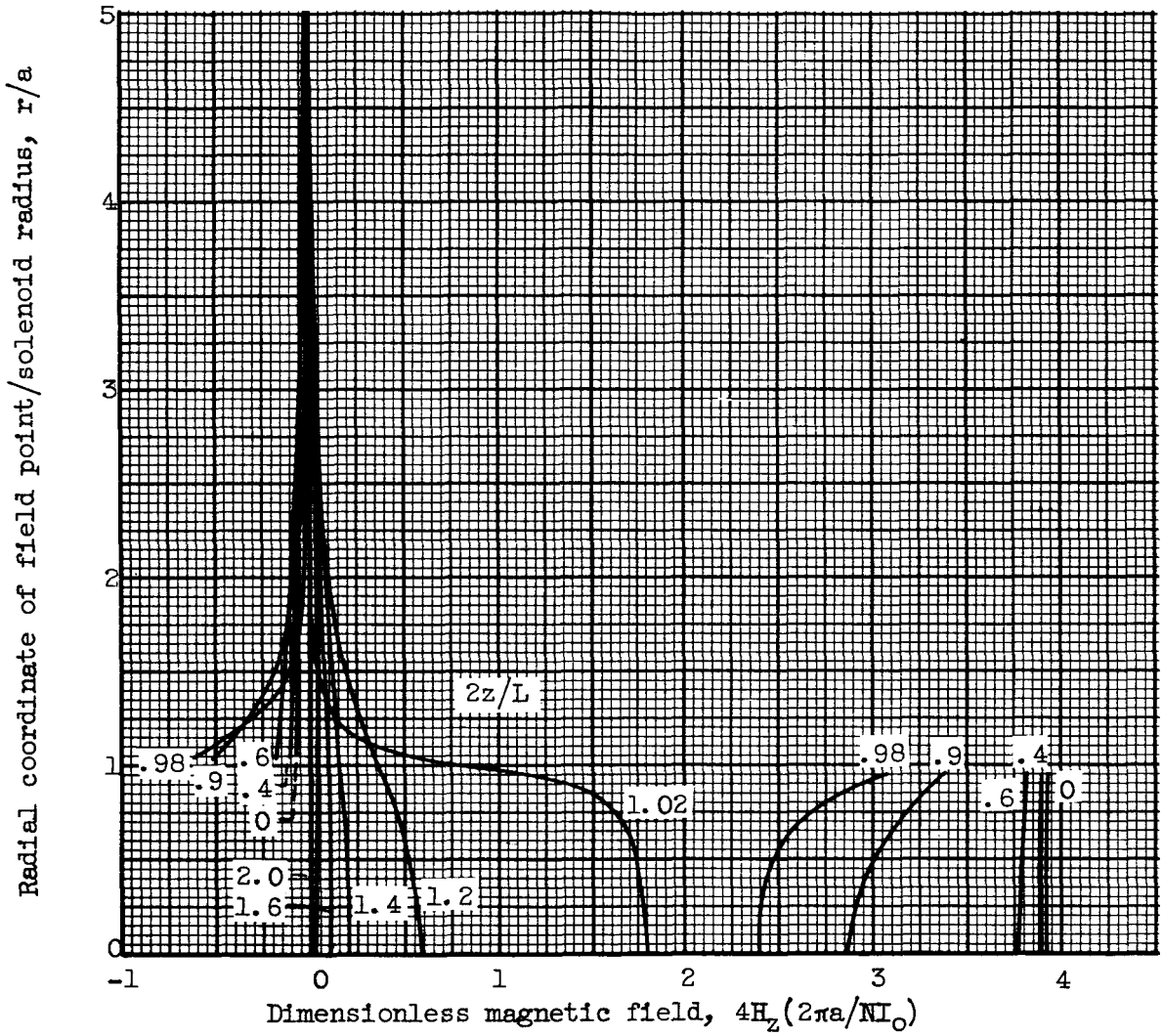

(o) Helical angle, 45.0°; length-radius ratio, 10.0.

Figure 3. - Continued. Dimensionless axial field of helical solenoid.

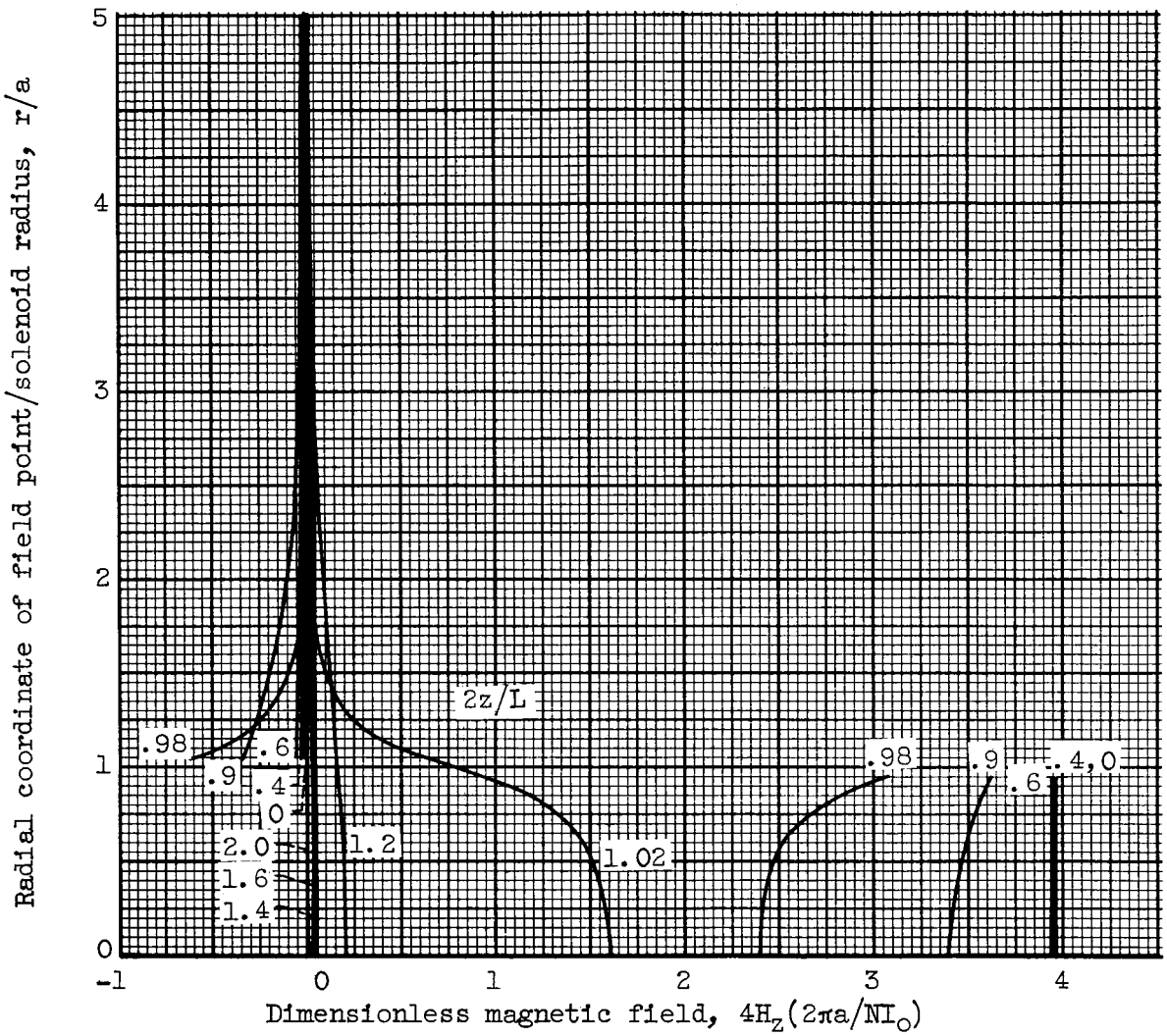

(p) Helical angle, 45.0°; length-radius ratio, 20.0.

Figure 3. - Concluded. Dimensionless axial field of helical solenoid.

NASA-Langley, 1963 E-2122